DEVELOPMENT AND VERIFICATION OF AN EXCEL PROGRAM FOR CALCULATION OF MONITOR UNITS FOR TANGENTIAL BREAST IRRADIATION WITH EXTERNAL PHOTON BEAMS

THIS THESIS IS SUBMITTED TO THE

GRADUATE SCHOOL OF NUCLEAR AND ALLIED SCIENCES

DEPARTMENT OF MEDICAL PHYSICS

UNIVERSITY OF GHANA, LEGON

BY

MOLALGN GEBRESENBET WOLDEMARIYAM

(**10435671**)

IN PARTIAL FULFILMENT OF THE REQUIREMENTS FOR THE AWARD OF

MASTER OF PHILOSOPHY DEGREE

IN

MEDICAL PHYSICS

JULY, 2015

DECLARATION

This thesis is the result of research work undertaken by Molalgn Gebresenbet Woldemariyam in the Department of Medical Physics, School of Nuclear and Allied Sciences, University of Ghana, under the supervision of Prof. A.W.K. Kyere, Prof. J.J. Fletcher and Mr. S.N. Tagoe.

…… ……

MOLALGN G.WOLDEMARIYAM DATE

(STUDENT)

…… ……

PROF. A.W.K. KYERE DATE

(PRINCIPAL SUPERVISOR)

…… ……

PROF. J.J. FLETCHER DATE

(CO-SUPERVISOR)

…… ……

MR. SAMUEL NII ADU TAGOE DATE

(CO-SUPERVISOR)

DEDICATION

To my parents, brothers, and sisters, in particular, to my dear mom, Eteye.

ACKNOWLEDGEMENT

Before all, I would like to thank the almighty God for his blessings and for choosing me to glorify his name through this research work.

I wish to thank and acknowledge the International Atomic Energy Agency (IAEA) and the government of Ethiopia for sponsoring my training in my dream field, medical physics.

My sincere gratitude goes to my supervisors Prof. A. W. K. Kyere, Prof. J.J. Fletcher and Mr. S.N. Tagoe for reading, reflecting, and giving advice to bring my thesis write up to its best form. Thank you Mr. Francis for sharing your tight time to read through my work and giving the valuable comments. I am grateful to Mr. Eric K. T. Addison of KNUST for letting me use their anthropomorphic phantom.

I would also like to thank my friends in SNAS: Tesfaldet Habtemariyam, Jemal Edris, Ainadine Ebrahimo Momade, Ignatius Komaketch….. Many thanks friends! Without your supports in various ways I couldn't imagine myself completing this thesis work.

Finally my deepest appreciation goes to the staff of the radiotherapy center of Korle-Bu Teaching Hospital (KBTH) and Sweden Ghana Medical Center (SGMC), in particular, Mr. George Acquah, for being cooperative to any assistance requested.

LIST OF CONTENTS

LIST OF TABLES

Table

LIST OF FIGURES

Figure

LIST OF PLATES

LIST OF ABBREVIATIONS

2D	2 dimensional
3D	3 dimensional
DNA	Deoxyribonucleic Acid
SD	Standard deviation
MU	Monitor unit or treatment time
CT	Computed tomography
KBTH	Korle-bu Teaching Hospital
SGMC	Sweden Ghana Medical Center
TPS	Treatment Planning System
TG	Task Group
CPE	Charged Particle Equilibrium
TCPE	Transient Charged Particle Equilibrium
SSDL	Secondary Standard Dosimetry Laboratory
PSDL	Primary Standard Dosimetry Laboratory
IAEA	International Atomic Energy Agency
ICRU	International Commission on Radiological Units
ICRP	International Commission of Radiation Protection
AAPM	American Association of Physicists in Medicine
WHO	World Health Organization
TRS	Technical Report Series
SSD	Source Surface Distance
SAD	Source Axis Distance

QI	Quality Index
ISF	Inverse Square Factor
PDD	Percentage Depth Dose
TAR	Tissue Air Ratio
BSF	Back Scatter Factor
PSF	Peak Scatter Factor
TPR	Tissue Phantom Ratio
TMR	Tissue Maximum Ratio
OAR	Off Axis Ratio
WF	Wedge Factor
TF	Tray Factor
SAR	Scatter Air Ratio
SMR	Scatter Maximum Ratio
TCP	Tumor Control Probability
NTCP	Normal Tissue Complication Probability

ABSTRACT

The accuracy of MU calculation performed with Prowess Panther TPS (for Co-60) and Oncentra (for 6MV and 15MV x-rays) for tangential breast irradiation was evaluated with measurements made in an anthropomorphic phantom using calibrated Gafchromic EBT2 films. Excel programme which takes in to account external body surface irregularity of an intact breast or chest wall (hence absence of full scatter condition) using Clarkson's sector summation technique was developed. A single surface contour of the patient obtained in a transverse plane containing the MU calculation point was required for effective implementation of the programme. The outputs of the Excel programme were validated with the respective outputs from the 3D treatment planning systems.

The variations between the measured point doses and their calculated counterparts by the TPSs were within the range of -4.74% to 4.52% (mean of -1.33% and SD of 2.69) for the prowess panther TPS and -4.42% to 3.14% (mean of -1.47% and SD of -3.95) for the Oncentra TPS. The observed degree of deviation may be attributed to limitations of the dose calculation algorithm with in the TPSs, set up inaccuracies of the phantom during irradiation and inherent uncertainties associated with radiochromic film dosimetry.

The percentage deviations between MUs calculated with the two TPSs and the Excel program were within the range of -3.45% and 3.82% (mean of 0.83% and SD of 2.25). The observed percentage deviations are within the 4% action level recommended by TG-114. This indicates that the Excel program can be confidently employed for calculation of MUs for 2D planned tangential breast irradiations or to independently verify MUs calculated with another calculation methods.

CHAPTER ONE

1. Introduction

1.1 Background

Cancer is a leading cause of death worldwide, accounting for 8.2 million deaths in 2012 alone. Based on projections for 2015, an estimated 15.2% of all deaths worldwide will be due to cancer [1]. Along with biologic therapies, surgery, chemotherapy, oxygen, and heat, radiation therapy (radiotherapy) is one of the most important methods of cancer treatment [2]. At least 50 percent of all cancer patients will receive radiotherapy at some stage during the course of their illness [3]. It uses ionizing radiation to kill cancer cells by damaging their DNA. External beam radiation therapy is the most common form of radiation therapy and is the main concern of this work. In external beam radiation therapy a source of radiation at some distance from outside of a patient's body aims radiation at cancer cells. Internal beam radiation therapy (brachytherapy) is the other form of radiation therapy where radiation is put inside the patient's body, in or near the cancer cells.

In external beam radiation therapy, treatment planning is a process which generates the treatment parameters considered optimal in the management of a patient's disease. These parameters include the target (tumor) volume, the organs at risk, number, orientation and shape of the radiation beam, positioning of the patient, dose distribution and beam on time. Determination of the parameters and their accuracy depends on the type of treatment planning used. In 2D treatment planning, determination of the optimal number, direction and shape of the radiation beam is determined on a conventional simulator, an

x-ray machine that has the same geometric and mechanical properties as the actual treatment machine. Dose calculation is based on a single transverse contour information through the central axis of the radiation beam or based on an assumption that the patient's body is flat and homogeneous. 3D treatment planning, on the other hand, is solely based on CT information and a software specifically designed for treatment planning, treatment planning system (TPS). Determination of the optimal beam direction, size and shape is done by a process known as virtual simulation with the TPS. In the process digitally reconstructed radiographs (DRRs), to visualize the target volume and normal structures superimposed on the beam defining collimators are produced. This is done by tracing ray lines from a virtual source position through the CT data of the patient to a virtual film plane and simulating photon attenuation. The CT data also provide high resolution internal density and external contour information that is necessary for correcting for heterogeneities and surface irregularities for accurately calculating dose using the dose calculation algorithm in the TPS.

The ultimate goal of treatment planning is to tailor delivery of the highest possible dose to the target volume, whilst minimizing the dose to normal tissues as much as possible. To achieve this goal each link in the "radiotherapy chain" (calibration of the treatment machine, the different stages of the treatment planning process, dose delivery, final quality assurance (QA), etc.) must be carefully and optimally performed. This thesis examines the dose calculation link in this chain as it applies to MU calculation for tangential breast irradiation. Monitor unit (MU) is a setting on a clinical linear accelerator unit to control the amount of radiation dose delivered to the patient. In this work MU also applies to the treatment time settings on Co-60 units.

Conventional 2D monitor-unit or treatment time (MU) calculation methods failed to routinely agree with 3D treatment planning systems (TPS) within reasonable range in calculating MU for tangential breast irradiation. This is because conventional MU calculation methods inherently assume full scatter condition which is not realized during irradiation of an intact breast or chest wall with parallel opposed tangential beams. 3D TPSs are able to account for the loss of full scatter condition in the dose computation process, but this needs to be ascertained or confirmed with measurement.

1.2 Statement of the problem

Currently the radiotherapy center of Korle-Bu Teaching Hospital (KBTH) and Sweden Ghana Medical Center (SGMC) are implementing 3D treatment planning using Prowess Panther and Oncentra treatment planning systems respectively. Both TPSs have a dose calculation algorithm based on superposition-convolution method. The accuracy of the dose calculation algorithms are validated for standard irradiation geometries (normal beam incidence on a flat water phantom affording full scatter conditions) during commissioning. However, it is recommended by several authors [4]–[6] that the accuracy of dose calculation algorithms to be tested for irradiation geometries that deviate significantly from that of standard irradiation geometry. Irradiation of intact breast or chest wall with tangential fields is one such geometry.

Despite the improved accuracy with 3D treatment planning, KBTH still uses 2D treatment planning for different reasons, for instance, when the patient cannot afford to have a CT scan. Calculation of MUs for this 2D plans is based on an assumption that the patient has a flat topography and offers full scattering conditions, i.e. it assumes that

scattered dose will be contributed to the calculation point from the entire part of the radiation field size irradiating the treatment volume. During breast irradiation with tangential beams however, there is a loss of full scattering condition due to the creation of a significant amount of "missing tissue" as a result of the presence of "air splash", oblique incidence of the radiation beam and the irregular surface contour of the breast (Plate 1.1). Therefore there would be overestimation of scattered dose at the calculation point and, hence, fairly large error may be introduced. MU calculations for breast irradiation should consider the loss of full scatter conditions for an improved accuracy, as a 1% higher accuracy results in 2% increase of success in radiotherapy [7].

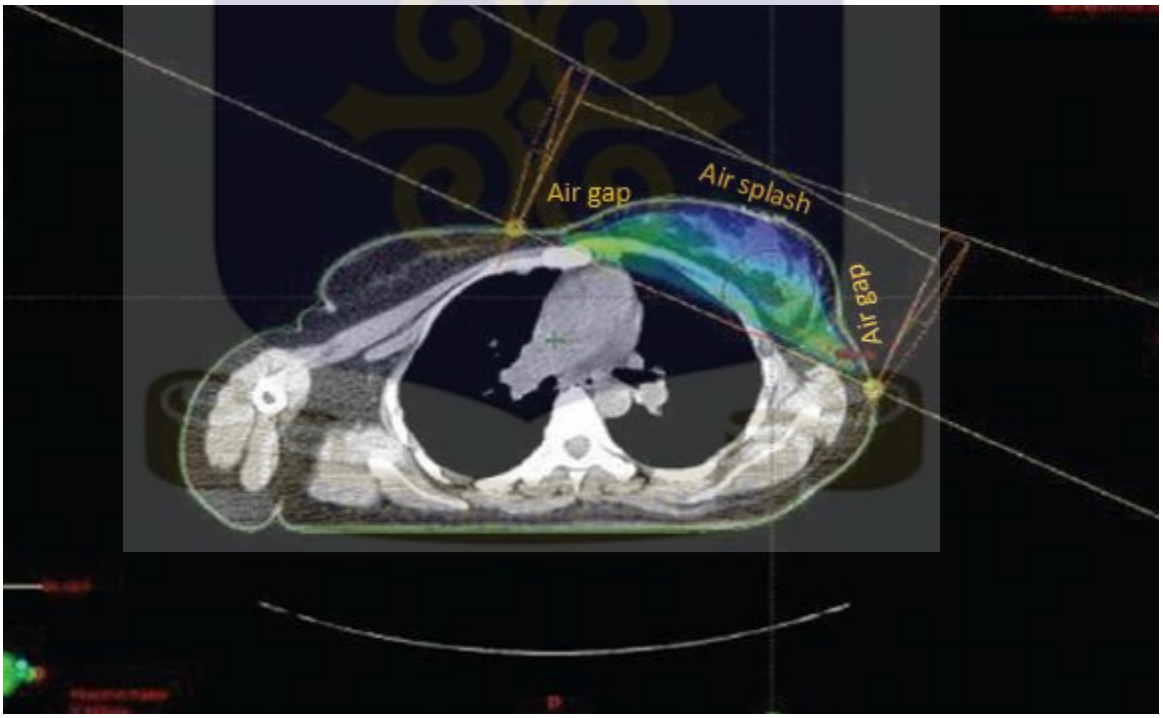

Plate 1.1: Irradiation of the left breast with medial and lateral tangential fields.

Several methods for correcting the overestimation of scattered dose during tangential breast irradiation by manual MU calculation methods have been developed [8]–[10]. The

methods are primarily designed to make manually calculated MUs agree with computer calculated ones. In addition they are based on assumptions and random reduction of the field size irradiating the breast volume.

Different professional groups have recommended second check of MUs with a calculation method that is independent from the original MU computation method [11]–[19]. When the secondary manual MU calculation methods available at KBTH and SGMC are applied to verify the MU calculations with the TPSs for tangential breast plans, for most of the times, they fail to agree within the recommended levels (5% [20]). This is due to the secondary MU calculation methods not accounting for MU calculation points being at off-axis points and loss of full scattering conditions due to the irradiation geometry.

1.3 Objectives

The overall objective of this work is to develop an Excel program for calculation of MU for tangential breast plans and for validation of the program by comparison with MU computations with 3D TPSs, which will first be validated with measurements made in an anthropomorphic phantom. The specific objectives regarding the mathematical model used by the calculation method are:

- Developing an algorithm for calculation of effective equivalent square field size that will take into account the loss of full scatter condition based on Clarkson's sector summation technique of differential scatter air ratios.

- Building an algorithm for calculation of MU required to deliver a certain amount of dose to a point in tangential breast irradiation based on look-up of data from tables of dosimetric functions.

In relation to validation of the MU calculation program and the treatment planning systems at KBTH and SGMC the following are the specific objectives:

- To verify the accuracy of MU calculations with Prowess Panther and Oracle treatment planning systems for tangential breast irradiation by comparison with measurements made in anthropomorphic phantom with calibrated radiochromic films.
- To validate the accuracy of the MU calculation program by comparison with computation outcomes from the above mentioned treatment planning systems.

1.4 Scope and delimitations

The MU calculation method presented in this work will apply only to the calculation of MUs for tangential irradiation of the breast or chest wall with external and static Co-60, 6MV and 15 MV photon beams. The calculation method will be based on a single two dimensional external contour and field border information. While the calculation method accounts for loss of full scattering condition due to air splashes and contour surface irregularity, accounting for the presence of heterogeneity such as lung is beyond the scope of this work. In addition the method is for calculation of dose at a single point in the central part of the radiation beam, it does not apply for calculation of dose distribution or calculations of dose at points in buildup or penumbra regions. Validation of the accuracy of point dose calculations with the dose calculation algorithms of the TPSs will

be performed only for points well within the irradiated volume, consideration of doses at points within heterogeneities and high dose gradient regions will not be covered.

1.5 Relevance and justification

In emergent radiotherapy cases and under situations where, due to different reasons, it is not possible to calculate MUs for intact breast and chest wall tangential fields as part of a computerized treatment plan, the MU calculation program from this work may give MUs calculated with a better accuracy level than MUs calculated based on standard irradiation geometry assumption.

The MU calculation method developed from this work can be used as a verification tool for second checking of MUs calculated by TPSs to ensure that the TPS calculation is accurate enough for the safe and effective treatment of the patient.

As part of the research work is to verify the accuracy of the MU calculation method by comparison with TPS calculations and measurements, the accuracy of the dose calculation algorithms used in Prowess Panther and Oracle treatment planning systems, at KBTH and SGMC respectively, will be first checked against measurements performed in a configuration that simulates clinical breast irradiation. This is in line with the recommendations of several publications [6], [14] that the accuracy of dose calculation algorithms should be verified with measurement for a variety of test cases.

CHAPTER TWO

2. Literature review

2.0 Introduction

The main aim of this chapter is to review the literature that is relevant to the focus of this work. Starting with introductory sections on dosimetric terms and devices, it continues with absolute dose determination under reference conditions (calibration). This will be followed by a brief description of the different types of dose calculation algorithms and principles of correction based MU calculation method. Next, the need of accuracy in radiotherapy together with accuracy requirements of dose calculations systems will be presented. Finally some previous works on 2D methods to account for the absence of full scattering conditions and validation of the accuracy of TPS calculated MUs for breast irradiation will be presented.

2.1 Radiation dosimetry and types of dosimeters

The mean energy (dE) imparted by ionizing radiation to matter of unit mass (dm) is defined as absorbed dose (D) by ICRU [21]:

$$D[Gy] = \frac{dE[J]}{dm[Kg]} \qquad (2.1)$$

Gray (Gy), the unit of absorbed dose, is not a measure of quantity of radiation but rather it relates radiation to its biological impact on the irradiated material [22]. Radiation dosimetry deals with quantitative determination of absorbed dose (or simply dose) in a medium.

Dosimetry may be performed for different goals including: commissioning of radiation therapy machines and treatment planning systems; periodic QA to check whether the commissioning dosimetry remains valid; treatment planning QA to guarantee that the calculated dose and dose distribution are accurate; to determine dose in regions where dose calculation algorithms are less accurate (dose build up region, sharp boundary between different absorbing materials) [23].

A dosimeter (sometimes termed a detector) is a device for measuring absorbed dose. Some of the commonly used dosimeters are mentioned below. In all cases the dosimeter, via calibration, yields the absorbed dose to its own sensitive volume from a measurement of charge, film blackening, light, etc., depending on the type of dosimeter [24].

Many characteristics of a dosimeter should be considered before using it for a specific application. The desirable dosimeter properties include accuracy and precision, linearity, dose or dose rate dependence, energy response, directional dependence and spatial resolution [25].

2.1.1 Ionization chambers

An ionization chamber is a gas filled cavity enclosed by a conductive outer wall and having a central collecting electrode [25]. When the chamber is placed in a medium which is being irradiated charged particles produced by the radiation create ionization inside the chamber while passing through it. An electrometer connected to the chamber applies voltage across the wall and the central electrode to collect and measure the charge.

The dose deposited in the gas can be calculated from the measured ionization (charge) using the equation:

$$D_{gas} = \frac{Q}{m_{gas}} W \qquad (2.2)$$

Where Q is the ionization produced in coulombs, m_{gas} is the mass of the gas inside the cavity, and W is the average energy required to produce one ionization in gas (33.85 J/C, for air).

Conversion of D_{gas} to dose absorbed by the medium (D_{med}) is based on Bragg-Gray cavity theory [26], [27] and its further improvements[28], [29]. Accurate conversion of the dose in the detector material to the dose in medium the well-known Bragg-Gray cavity situation must be fulfilled by the chamber. In order for a detector (cavity) to be treated as Bragg-Gray cavity, the cavity must not disturb the charged particle fluence (including its distribution in energy) existing in the medium in the absence of the cavity. A small (< 1 cm^3) air filled thimble type ionization chamber with thin walls can be approximated to be considered as Bragg-Gray cavity and is recommended as a reference tool of clinical dosimetry.

Cylindrical (thimble type) and parallel plate (plane parallel) ionization chambers are the two types of cavity chambers. They are mostly open and therefore require temperature and pressure corrections to account for the change in the mass of air in the chamber volume, which changes with the surrounding temperature and pressure [25].

2.1.1.1 Monitoring ionization chambers

A monitor chamber (or simply monitor) is a type of ionization chamber (parallel plate) that is placed in the head of Linac to control dose delivery. The current produced in the chamber by the radiation is related to the actual dose rate being given to the patient. The amount of charge produced in the chamber associated with 1cGy in the standard irradiation conditions is defined as one monitor unit (MU). To avoid reading variations due to changes in temperature and pressure, these chambers may be sealed. The MU required to deliver a treatment dose is calculated and set on the Linac and the combined current signal from the chamber is used to terminate the generation of radiation upon completion of delivering the required dose [24].

2.1.2 Semiconductor detectors.

2.1.2.1 Diodes

A diode is a P-N junction, it is formed by joining P type semiconductor with N type semiconductor. In an isolated diode the net current is zero since diffusion current (diffusion of majority charge carriers in the space charge region in the direction of the diode) is equal to drift current (flow of minority charge carriers in the opposite direction of the diode due to the electric field in the space charge region).

Ionizing radiation produces free electrons and holes in the body of the diode increasing the number of minority carriers and therefore a net current is generated in the reverse direction in the diode. The magnitude of the current is proportional to the energy deposited by the radiation.

Diodes can operate without an external bias and can be made very small to give good spatial resolution without compromising sensitivity [30].

2.1.2.2. MOSFETs

Metal-Oxide Semiconductor Field Effect Transistor (MOSFET) is the other type of semiconductor dosimeter. There are two types of MOSFET; PMOS and NMOS. PMOS is manufactured by joining two P type semiconductors with an N type semiconductor in the middle. The N type creates a barrier preventing flow of charge carriers (holes) between the two P type regions. An insulator (Silicon dioxide) is placed on top of the N type and a highly conducting material is placed over the insulator. A negative voltage applied to the conductor repels electrons and attracts holes in the N type region inducing a P type region at the edge of the silicon dioxide. As the voltage increases in magnitude the concentration of holes in the induced P type region increases until eventually it can support a measurable current between the two P type regions. This level of the voltage that results in the significant increase in current is called threshold voltage.

Irradiation of the body of MOSFET dosimeter with ionizing radiation produces charge that is permanently trapped in the silicon dioxide. This results in change in the threshold voltage. Dosimetry with MOSFETs is based on measurement of the change in threshold voltage which is a linear function of absorbed dose [25].

MOSFETs have excellent spatial resolution and do not attenuate the beam significantly due to their small size, which is particularly useful for in vivo dosimetry.

2.1.3 Luminescence dosimeters

Luminescence is a phenomenon in which certain crystalline materials, when stimulated by heat or light, release light that is proportional to the radiation dose to which they have been irradiated previously [31]. Thermolominescent dosimetry (TLD) is when heat is used for stimulation. The technique of determination of absorbed dose from measurement of emitted light using light as a stimulant is called optically stimulated luminescence dosimetry (OSL).

Luminescent dosimeters are mostly made from lithium fluoride (LiF). Pure LiF has a crystalline structure with allowed and forbidden energy bands. When impurities are added imperfections arise in the lattice structure creating energy traps in the forbidden region. Upon irradiation some of electrons of LiF are excited to higher energy levels. Most of the electrons immediately return to the ground state, but a few remain trapped in the impurity levels (metastable state). If there is spontaneous emission of light owing to transition from the trap to ground state, this is called fluorescence. If an electron requires external energy to return to the ground state, the emission of light in this case is called phosphorescence. Upon heating or absorption of light the trapped electrons are raised to still higher energy state from which they can return to the ground state[31], [32].

Luminescence dosimeters are most widely used in radiotherapy due to their tissue equivalence and high sensitivity.

2.1.4 Films

2.1.4.1 Radiographic films

A radiographic film is prepared by coating a transparent film base (cellulose acetate or polyester resin) with emulsion of silver bromide crystals. When the film is irradiated with ionizing radiation or light, electrons within in the emulsion become exited and neutralize mobile Ag^+ ions. The exited electrons attract and neutralize the silver ions and metallic silver is deposited. The neutralization of silver ions is called latent image because it is invisible. When the film is placed in a developing solution, the latent image catalyzes further deposition of metallic silver. When the film is put inside a fixing chemical the silver bromide that was unaffected by the radiation will be removed [33].

The amount of deposited metallic silver (the degree of blackening of the film) is proportional to the absorbed dose and can be measured by determining the optical density or absorbance of the film. Optical density (OD) of the film is measured by directing a light of intensity (I_0) through the film and determining the transmitted light intensity (I):

$$OD = \log\left(\frac{I_0}{I}\right) \qquad (2.3)$$

The quantity I/I_0 is the fraction of light transmitted through the film or transmittance (T). Therefor OD can be related to T as:

$$OD = \log\left(\frac{1}{T}\right) \qquad (2.4)$$

Strengths of radiographic film include high contrast, high spatial resolution and high sensitivity. Being sensitive to room light, requirement of wet chemical processing and not

being tissue equivalent in terms of photon energy absorption and scattering are limitations of radiographic films[34].

2.1.4.2. Radiochromic film

The shortcomings of radiographic films mentioned in the above section have been solved with the introduction of radiochromic films. Radiochromic films do not require chemical processing, they color directly upon exposure to ionizing radiation. They are unresponsive to visible light and they simulate the radiation absorption properties of muscle and water. Furthermore they have very high spatial resolution and they exhibit little sensitivity variation with photon energy [34], [35].

The most commonly used type of radiochromic film is Gafchromic ® film [36].There are different types of Gafchromic ® film including EBT2, EBT, MD-55-1, and MD-55-2. EBT2 film will be used in this work.

The structure of EBT2 Gafchromic ® film is shown in Figure 2.1. It consists of an active layer (30µm thick) on top of which a 5µm topcoat is attached. A clear polyester laminate of 50µm thickness is glued over the topcoat with a 25µm thick pressure sensitive adhesive. Beneath the active layer is a clear polyester of thickness 175µm for lamination. The polyester surfaces make the film water proof, allowing the insertion of the film in to water[37].

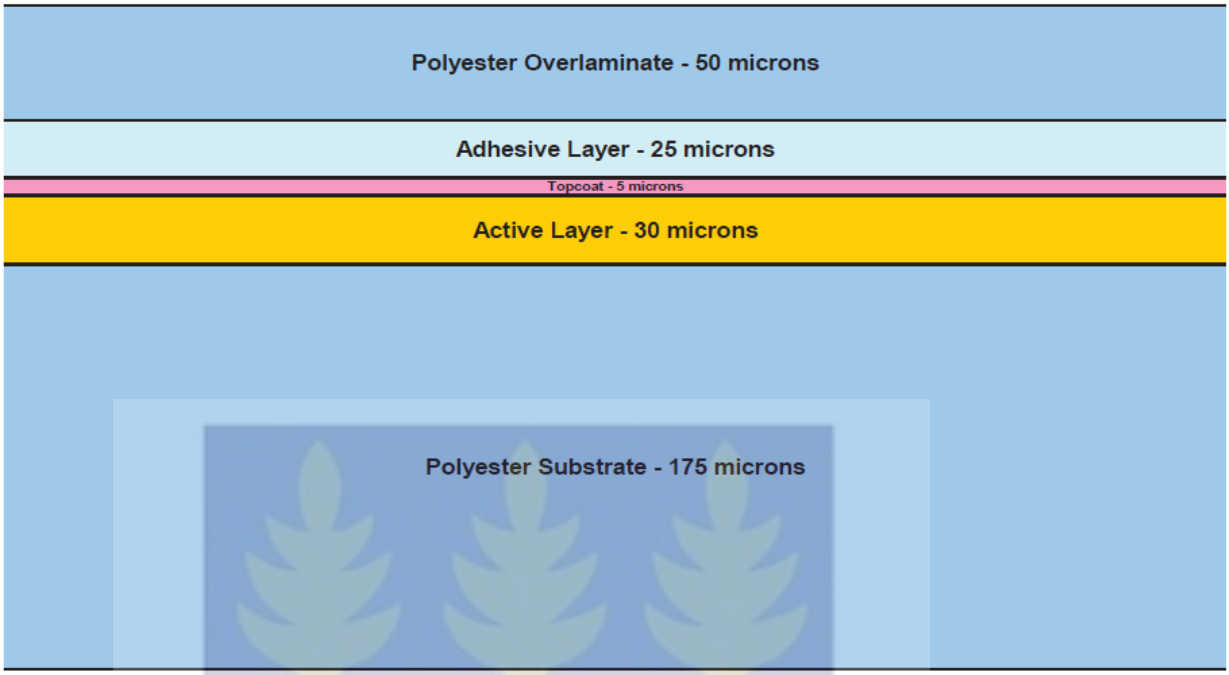

Figure 2.1: Configuration of EBT2 Gafchromic® film.

The appearance of unirradiated EBT2 films is yellow due to the presence of a yellow dye in the active layer to decreases UV/light sensitivity. When the film is irradiated, photons and charged particles transfer energy to the colorless photomonomer molecules in the active layer, initiating a dye forming or polymerization process, resulting formation of blue colored polymer [34]. As a result the original yellow colored film becomes green (blue color inside yellow film appears green). Optical density (OD) is the measure of the greenness of the film which in turn is proportional to dose. When the irradiated film is scanned, the scanner measures the fraction of light transmitted through the film or transmittance (T). Optical density can be obtained from transmittance using equation (2.4). However in this thesis transmittance (pixel intensity value) will be related directly to dose.

2.1.4.3 Dosimetry with Gafchromic® films

Some authors, [34], [37] have specified different recommendations related to dosimetry with radiochromic films, the following is summary of the recommendations:

- Films should be cleaned with lintless paper before use and gloves should be worn to handle them
- Exposure to sunlight should be avoided. The film may be stored at room temperature (20º– 25º C), but the best practice is to store the film at refrigerator temperature.
- Gafchromic® EBT2 film is designed to be handled in interior room light, however it is recommended that the film be kept in darkness when it is not in use.
- The time interval between the exposure and the scan should be kept approximately the same for all films in an analysis.
- The response of EBT2 film is sensitive to the orientation of the film in the scanner. It is recommended that EBT2 film is scanned in landscape mode.
- The sensitive emulsion layers of radiochromic films absorb most strongly in the red wavelength, about 660 nm region. Thus the densitometer response is optimized at these wavelengths.

2.2 Absolute dose measurement under reference conditions (Calibration)

Before a treatment machine is used for patient treatment there is a need to establish the accurate relationship between a reading on the dose delivery control system of the machine and the absolute dose delivered by the machine to a point at a reference depth in

a water phantom under reference irradiation conditions. This process is known as calibration.

In cobalt units dose delivery is controlled by a timer. Calibration of cobalt units involves determining and verifying the absolute dose delivered by the unit under reference conditions for a "treatment time" of a certain duration on the timer. This gives the dose rate in cGy/min at the point at the normalization depth under the reference irradiation conditions.

For linear accelerators it is usual to have an ionization chamber, called monitoring ionization chamber, situated in the beam close to the X-ray source. This gives a reading in monitor units (MU) proportional to the dose delivered by the beam. Conceptually MU is not different from treatment time for cobalt units therefore in this thesis MU is used also in place of treatment time. Calibration of a Linac consists in setting and maintaining the reading of the monitor ionization chamber to 1 MU when 1cGy is delivered to the point at the normalization depth under the reference irradiation conditions.

In routine clinical practice, to measure absorbed dose at a reference point in water, a code of practice is followed, based on the use of an ionization chamber having a calibration factor, traceable either directly to primary standard dosimetry laboratory (PSDL) or to secondary standard dosimetry laboratory (SSDL), itself, in turn linked to a PSDL. In a SSDL calibration of ionization chambers is carried out in the Co-60 beam under environmental conditions of 20^0C temperature and 101.3 kPa atmospheric pressure. Therefore a correction is required if measurement of dose is done under different temperature and pressure conditions for different beam quality. The absorbed dose in water at the reference depth for radiation of quality Q given by:

$$D_{w,Q} = M_{raw} \cdot N_{D,w} \cdot K \,.K_Q \qquad (2.5)$$

Where M_{raw} is the reading of the electrometer in Coulombs (C) and $N_{w,Q}$ is the calibration factor of the chamber for dose absorbed in water given in the dosimetric code of practice. The calibration factor for an ionization chamber is valid only for the reference conditions and for the type of radiation used during calibration of the chamber at the SSDL. Any departure from the reference conditions when using the ionization chamber in the user beam is accounted for by the correction factors K and K_Q. K accounts for various measurement conditions that are different from the reference conditions and is given by:

$$K = K_{TP} \cdot K_{ion} \cdot K_{pol} \cdot K_{elec} \qquad (2.6)$$

Where K_{TP} is the temperature–pressure correction factor which corrects the reading to the standard environmental conditions for which the ion chamber's calibration factor applies; K_{ion} corrects for incomplete ion collection efficiency; K_{pol} corrects for any polarity effects; and K_{elec} takes into account the electrometer's calibration factor if the electrometer and ion chamber are calibrated separately.

Currently the radiotherapy center of Korle-bu teaching hospital and Sweden Ghana Medical Center are using TRS-398 [38] and TG-51[39] respectively which are code of practices given by IAEA and AAPM respectively for absolute dose determination under reference conditions (calibration). Both TRS-398 and TG-51 recommend the use of either SSD or SAD arrangement of the treatment machine, the water phantom, and the ionization chamber for the calibration process. SAD stands for source axis distance and it is the distance between the radiation source and the isocentre. Isocentre of a radiotherapy machine is the point where the axis of rotation of the beam collimating system of the

machine intersects with the axis of rotation of the treatment head of the machine (Figure 2.2). SSD stands for source surface distance. It is the space between the radiation source and the surface of the phantom or the skin of a patient. In SAD calibration setup the detector is placed at the isocentre and in SSD setup the surface of the phantom is placed at the isocentre distance and the detector will be at some depth inside the phantom (Figure 2.2).

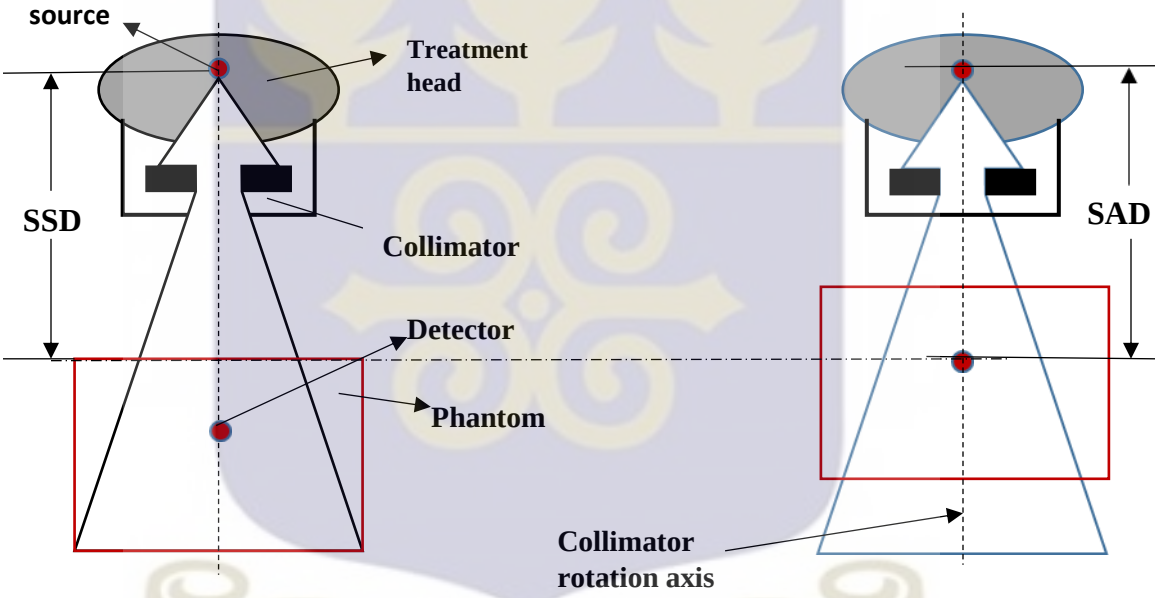

Figure 2.2: SSD and SAD calibration set ups

2.3 Monitor unit calculation for external photon beams

2.3.1 Dose calculation algorithms

The intent of dose calculation algorithms is to predict the dose (or dose rate) delivered to any point within the patient with as much accuracy as possible [40]. The three major dose

calculation algorithms that exist today are: correction based, convolution-superposition, and Monte-Carlo algorithms[41].

Correction based (also called factor based or semi empirical methods) are based on tabulated data measured in a water phantom. To correct for the clinical irradiation condition and patient characteristics the beam is reconstituted using "Clarkson summation" or a similar technique [31], [42], [43]. In this thesis a correction based calculation method is used and the method will be discussed in more detail in the latter sections.

In convolution-super position algorithms the radiation beam is modelled from its energy fluence (amount of energy crossing unit area) as a collection of many parallel pencil beams. Each pencil beam contributes dose at points both near to and far from the axis of the pencil. The function which expresses the dose as a function of depth and distance from the axis of the beam is called a kernel. Kernels are usually pre calculated using Monte-Carlo simulation. Finally, the dose is given by adding the dose contribution from all pencil beams for each volume element of the irradiated volume and this process is known as 'convolution-superposition' [40], [41], [43], [44].

The Monte-Carlo method is the most accurate method for dose calculations in heterogeneous media. It explicitly simulates the transport of photons and particles using the first principles of physics and applies exactly the statistical nature of interaction of radiation with matter by using microscopic cross sections that govern different interactions (photoelectric effect, Compton scattering, pair production, etc.) Dose deposition is computed by accumulating (scoring) ionizing events in bins (voxels) [32], [45].

Regardless of the type of dose calculation algorithm implemented, the basis for determining the MU required to deliver the prescribed dose to the patient is to arrive at the dose per MU or dose rate ($\dot{D}$) at the point of interest in the patient from the dose rate measured under the reference calibration conditions ($\dot{D}_R$). It should be noted that $\dot{D}$ is to be evaluated at some depth (Z) in the patient for irradiation parameters (C) and $\dot{D}_R$ is measured at the reference depth (Z_R) inside a water phantom under irradiation parameters (C_R), i.e.:

$$\dot{D} = \frac{D(Z,C)}{MU} \qquad (2.7a)$$

$$\dot{D}_R = \frac{D(Z_R,C_R)}{MU} \qquad (2.7b)$$

From the two equations above one can write:

$$\dot{D} = \dot{D}_R \frac{D(Z,C)}{D(Z_R,C_R)} \qquad (2.8)$$

The methodology to drive the factor $\frac{D(Z,C)}{D(Z_R,C_R)}$ varies among the different dose calculation algorithms. In correction based dose calculation methods the factor represents experimental data. In fluence based calculation methods (superposition-convolution and Monte Carlo), the factor is obtained from calculations[43].

2.3.2 Correction based MU calculation and dosimetric functions

In correction based MU calculation methods the ratio $\frac{D(Z,C)}{D(Z_R,C_R)}$ is obtained by measuring dose rate for a wide range of conditions representative of the clinical use and relate these

measurements to absolute dose by normalizing them to the reference (calibration) conditions. The term relative dosimetry is given to all measurements, which are compared to the dose at the absolute calibration point. Dosimetric quantities (functions) that are measured in this manner will be discussed next.

2.3.2.1 Percentage depth dose (PDD)

PDD interrelates doses at two points at different depths along the central axis of the beam. It is defined as the quotient, expressed as a percentage, of the absorbed dose at any depth d to the absorbed dose at a fixed normalization depth d_0, along the central axis of the beam[32]. The reference depth is often the depth of maximum dose but can actually be at any chosen depth[31].

$$PDD(d, w_m, F, E) = 100 \times \frac{D_d}{D_{d_0}} \qquad (2.9)$$

PDD depends on the depth d, the width of the field size at the normalization depth, w_m, the distance of the phantom surface from the radiation source and on the quality of the radiation. Therefore, PDD data for a given beam energy is usually collected for several square fields and depths and the water surface at the standard source to surface distance (usually 100 cm) [24]. However the majority of fields used in radiotherapy are rectangular or irregularly shaped and in isocentric patient setup, the patient's skin surface is not at the standard SSD. Therefore in order to use PDD data for calculating dose at a given depth from a known dose at the normalization depth for such situations a system of relating square fields to different field shapes and converting PDD data from one SSD to another is required.

In order to use tabulated PDD data for rectangular or irregularly shaped fields the concept of equivalent squares or equivalent circle will be used. A simple rule-of thumb method by Sterling [46] states that a rectangular field is equivalent to a square field if they have the same area to perimeter ratio. Therefore the side length *l* of the equivalent square field of a rectangular field of width *a* and length *b* is:

$$l = \frac{2ab}{a+b} \qquad (2.10)$$

Equivalent circle is one that has the same area as the equivalent square. Hence the radius r of the equivalent circle of a rectangular field of width *a* and length *b* is:

$$r = \frac{8ab}{\sqrt{\pi}\,(a+b)} \qquad (2.11)$$

When using PDD data measured at a standard SSD for dose calculations for treatment of patients with another SSD, it is necessary to make a correction to the PDD data measured at another SSD.

2.3.2.2 Tissue-air ratio (TAR)

Since PDD tables for clinical use are usually measured at a standard SSD, their application to patient treatments at a different SSD needs correction and this might be cumbersome in routine clinical practice. The dosimetric quantity TAR avoids this SSD dependence, a single TAR table can be used for all source distances that may be encountered in clinical situations.

TAR is defined as the ratio of dose in water measured at depth d, where the field size is A_d and from there the source is at distance equal to $SSD + d$, on the beam central axis in

a large phantom, to the dose to water measured in air for the same collimator opening and at the same distance from the source:

$$TAR(d, A_d, E) = \frac{D(d, A_d, SSD)}{D(Air, A_d, SAD)} \quad (2.12)$$

TAR depends only on three parameters: depth d, field size A_d at depth d and energy of the beam E. Unlike PDD it does not depend on SSD for the range that is used clinically (50 – 100cm) [47].

2.3.2.3 Tissue-phantom ratio (TPR) and Tissue-maximum ratio (TMR)

Tissue-phantom ratio is defined as the ratio of the dose at a given point on the beam central axis in phantom for a given field size to the dose at the same point at a fixed reference depth for the same field size:

$$TPR(d, A_d, E) = \frac{D(d, A_d, SSD)}{D(d_{ref}, A_d, SSD + d - d_{ref}} \quad (2.13)$$

There is no a particular agreement on the reference depth to be used. However ICRU [42] has recommended a depth of 5cm for Co-60, 7cm for 1MV to 25MV X-rays, and 10cm for X-rays above 25 MV as a reference depth.

When the reference depth, d_{ref}, in equation 2.13 is chosen to be the depth of maximum dose, tissue-phantom ratio (TPR) becomes tissue-maximum ratio (TMR):

$$TMR(d, A_d, E) = \frac{D(d, A_d, SSD)}{D(d_{max}, A_d, SSD + d - d_{max}} \quad (2.14)$$

Like TAR both TPR and TMR are independent of surface to source distance.

2.3.2.4 Total scatter factor (S_{CP})

Total scatter factor (S_{cp}) is defined as the ratio of the dose for a given collimator defined field size A_c to that for the normalization collimator defined field size $A_{c,norm}$, both measured at the normalization depth d_{norm} in a full scatter phantom its surface is at the reference SSD. This quantity is also called in-water output ratio, relative dose factor, and field output factor.

$$S_{cp}(A_c) = \frac{D(d_{norm}, A_c, SSD)}{D(d_{norm}, A_{c,norm}, SSD)} \qquad (2.15)$$

When MU is calculated for open square and rectangular fields at the standard SSD, S_{CP} is the only quantity needed to account for both collimator and phantom scatter effects. However when blocked beams are used, when SSD different from the standard SSD is used or when there is a missing tissue in the beam, the direct use of S_{CP} to describe the field size dependence becomes inadequate and can cause a significant error. This is because the effects of the head scatter are then decoupled from the scatter conditions within the phantom for nonstandard irradiation geometries. This problem is avoided by decomposing S_{CP} in to collimator or head scatter factor S_c and the phantom scatter factor S_p [24].

2.3.2.5 Collimator scatter factor (S_c)

The collimator scatter factor (also known as head scatter factor or in air output factor), is defined as the ratio of the dose in air for a given collimator defined field size A_c to that for the reference collimator defined field size $A_{c,ref}$, i.e.:

$$S_C(A_C) = \frac{D(air,\ A_c, SSD)}{D(air, A_{c,ref}, SSD)} \qquad (2.16)$$

The need for S_c in MU calculations is to account for the variation of photon fluence with collimator settings.

2.3.2.5 Phantom scatter factor S_p

S_p accounts for the change in scatter radiation produced in the phantom at a reference depth as the field size is changed. It is defined as the ratio of the dose for a given field size A at the normalization depth d_{norm} in a phantom to the dose at the same depth for the reference field size (e.g., 10 × 10 cm), with the same collimator opening [32]. It is difficult to measure S_p according to its definition because of the difficulties associated with separately measuring the phantom scattered photons from the collimator scattered ones. Practically S_p is determined indirectly by employing the fact that S_{CP} contains both the collimator and phantom scatter and when divided by S_c yields S_p i.e.:

$$S_p(d_{ref}, A) = \frac{S_{cp}(A_c)}{S_C(A_C)} \qquad (2.17)$$

The field size argument of S_p indicates that S_p depends on the field size as it is defined by the normalization depth inside the patient as opposed to S_c, which depends on the collimator setting.

Since S_p and S_{cp} are defined at the normalization depth, when the normalization depth is chosen to be the depth of D_{max}, actual measurement of these factors at this depth may create problems because of the possible influence of contaminant electrons incident on the phantom. This can be avoided by making measurements at a greater depth (e.g., 10

cm) and converting the readings to the reference depth of D_{max} by using percent depth dose data [32]

2.3.2.5 Off-axis ratio (OAR)

The off-axis ratio (OAR) is defined as the ratio of dose at a point away from the central axis to the dose at the point on the central axis at the same depth:

$$OAR(x, A_d, d) = \frac{D(x, A_d, d, SSD)}{D(0, A_d, d, SSD)} \qquad (2.18)$$

OAR is a function of distance from the central axis *x*, depth d, and the field size A_d . A plot of the variation of OAR with distance *x* from the central axis is known as a beam profile. Beam profiles measured for different field sizes and at several depths are required for MU calculations. They are best obtained using a remotely controlled water phantom with its surface at the same SSD as for the PDD measurements[24].

2.3.2.6 Wedge transmission factor (WF)

Reference dosimetry is performed with open field, without any attenuating or scattering material between the source and the phantom. Actual patient treatment, however, may require the use of special blocks or absorbing filters placed in the path of the beam to modify the intensity distribution through the beam. The most commonly used beam-modifying device is the wedge filter. It is a wedge shaped metal block that causes a progressive reduction in the intensity across the beam. Wedges can be used to compensate for missing tissue in a sloping surface or, in the treatment of relatively low lying lesions, to allow beams to be brought in from two angled directions [25].

Three types of wedge filters are currently in use: physical, motorized and dynamic. A physical wedge (sometimes called external wedge) is an angled piece of lead or steel that is manually placed below the secondary collimators to produce a gradient in radiation intensity. A set of physical wedges (15°, 30°, 45°, and 60°) is usually provided with the treatment machine. A motorized wedge (or internal wedge), located above the secondary collimator jaws, is a physical 60^{o} wedge inserted into the field using a motorized drive within the head of the unit. Wedge angles smaller than 60^{o} are produced by a combination of wedged and open beams of appropriate proportion. Dynamic wedges are generated electronically by creating wedged beam profiles through dynamic motion of an independent jaw within the treatment machine.

Insertion of a wedge filter in to the path of the beam alters the radiation beam in different ways. First it removes low energy photons from the beam making the beam harder or more penetrating than the open field. Secondly it decreases the amount of radiation incident on the patient, which leads to reduction of dose rate on the central axis of the beam. [24].

Since characteristics of wedged beam is different from that of an open field it is important to measure all the dosimetric functions for the wedge independently and not to assume that it is the same as for the open field [48], [49]. Reduction of the beam intensity can be taken in to account by a factor called wedge transmission factor (WF), which is defined as ratio of dose rates measured with and without wedge at the central axis:

$$WF = \frac{\dot{D}(Wedge)}{\dot{D}(Open)} \qquad (2.19)$$

The wedge factor is sometimes incorporated into one of the dosimetric functions measured for wedged beam. In this case the dosimetric function is normalized relative to dose rate measured without wedge. Under this circumstance the wedge factor will not be applied independently[41], [50].

Another approach is to incorporate all the effects of putting a wedge filter into the path of the beam into the wedge factor. This approach avoids the need for separate wedge-field dosimetric functions, but may require wedge factors as a function of field size, depth, and off-axis distance. In this work the first approach, measuring dosimetric functions separately for wedged beams is followed.

2.3.2.7 Scatter air ratio (SAR) and scatter maximum ratio (SMR)

Because the scattered dose at a point in a phantom is equal to the total dose minus the primary dose at that point, the difference between TAR for a given field size and TAR for zero area field size has been called scatter-air ratio (SAR) [51], [52].

$$SAR(d, A_d, hv) = TAR(d, A_d, E) - TAR0(d, 0, E) \qquad (2.20)$$

Scatter-air ratios are used for the purpose of calculating scattered dose. For Co-60 beams, a table of SARs can be compiled from a TAR table using equation (2.20). For high energy linear accelerator beams, however, TAR data is not available due to the difficulties associated with measurement of TAR at these energies.

The scatter-maximum ratio (SMR), like the SAR, is a quantity intended specially for the calculation of scattered dose. SMR is the analogous scatter component for TMR as SAR was is for TAR. The relationship between TMR and SMR is given by Khan [32] as:

$$SMR(d, A_d) = TMR(d, A_d) \cdot \frac{S_p(A_d)}{S_p(0)} - TMR(d, 0) \qquad (2.21)$$

Where $S_p(A_d)$ and $S_p(0)$ are phantom scatter factors for a field size of A and zero respectively.

For Co-60 γ rays, SMRs are approximately the same as SARs. However, for higher energies, SMRs should be calculated from TMRs by using the above equation. In what follows SAR for Co-60 beams also applies to SMR for high energy beams.

2.3.3 Application of SAR (Cunningham's method of scatter computation using Clarkson's sector summation technique)

The reference dose rate, during calibration, is measured in a homogeneous water phantom with flat surface and large dimensions to provide full scatter condition. The radiation beam is also rectangular in shape and is incident perpendicularly on the flat phantom surface. The irradiated patient's body, however, could be non-homogeneous and/or irregularly contoured with the beam directed at an angle (tangential breast irradiation is a good example). This differences in composition and irradiation geometry result in attenuation and scattering differences relative to the reference conditions and therefore should be corrected in MU calculations. One way of accounting for the effects of loss of full scatter conditions and presence of herogenities is based on calculation of scattered dose to the calculation point [31], [32].

Cunningham's differential scatter air ratio (dSAR) method [52] can be used for calculation of scattered dose to a calculation point inside a medium with irregular surface contour. Figure 2.3 shows such a medium irradiated with a wedged field. The insert to the

figure shows the cross-section of the radiation field projected to the depth of the calculation point (point p). The transverse plane of point p is divided into sectors of angular width $\Delta\theta$. Each sector is further divided into area elements of dimension $r\Delta\theta\Delta r$ (point Q). Scattered dose from each element to the calculation point is represented by differential scatter air ratios (dSAR) as a function of depth of the element (d_Q), its radial distance from the calculation point (r) and its length (Δr).

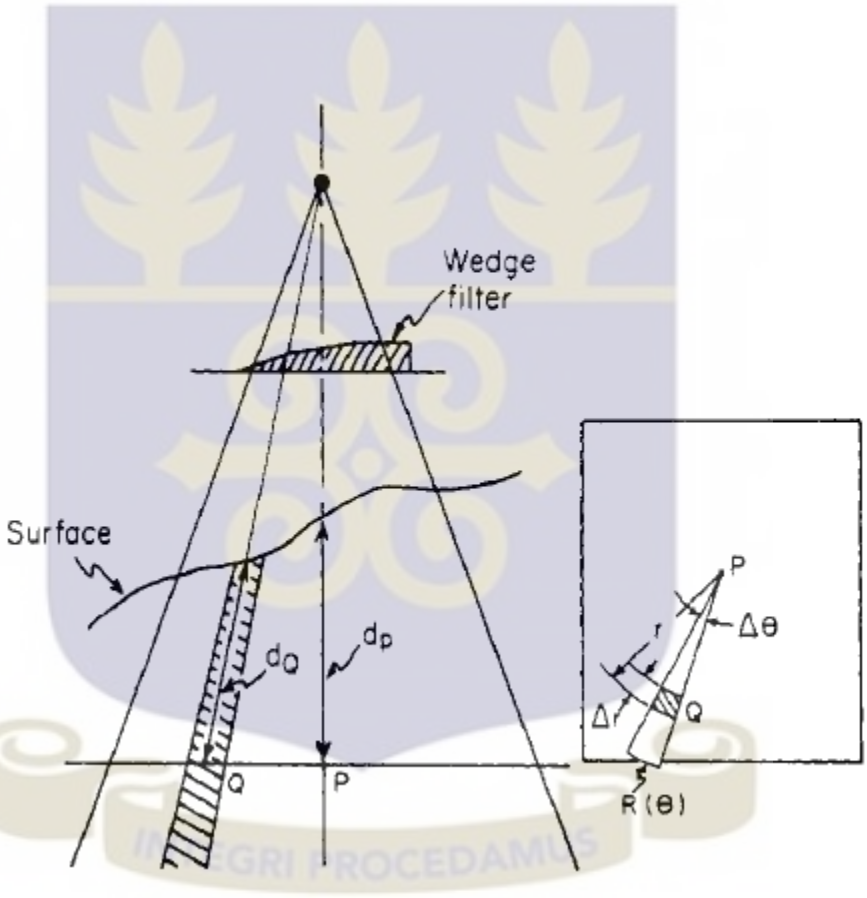

Figure 2.3: A diagram depicting scatter dose calculation at a point inside a medium with irregular surface contour.

Summation of scatter contribution from individual scatter elements is performed using Clarkson's sector summation technique[53]:

$$SAR = \sum_{i=1}^{n} \frac{\Delta\theta_i}{2\pi} \sum_{r=0}^{\infty} f(u,v) f_1(u,v) \left[SAR(d_Q, r) - SAR(d_Q, r - \Delta r) \right] \quad (2.22)$$

Where f_1 is a function to describe the scatter characteristics of the beam attenuated by the wedge as a function of the position of scattering element in the calculation plane. *u* and *v* are the horizontal and vertical coordinates of the scattering element (e.g. point Q in Figure 2.3) in the calculation plane, *f* is penumbra function to express the variation of scatter from a scattering element as a function of its distance from the central axis of the radiation beam.

In equation (2.22), summation of scatter from the scatter elements within each sector extends infinitely beyond the field boundary (R). However it needs to run only a short distance beyond the edge of the beam, because beyond the field edge *f(u,v)* would become very small.

The above technique of summation of differential scatter air ratios with respect to radial and angular increments can also be carried out with respect to depth, to account for heterogeneities in the medium of the calculation point. However inhomogeneity correction is beyond the scope of this work.

2.4. Accuracy required in radiotherapy

The principal problem in radiotherapy is that tumor cells are not treated in isolation. The tumor mass is always surrounded by normal tissue structures through which it may be necessary to direct the radiation beam. Therefore if the total dose given to a patient is increased, it is expected that both local tumor control and normal tissue damage will

increase. If this leads to a therapeutic advantage or failure depends on the steepness of the dose-response curve for the tumor and the surrounding normal tissue. Dose-response curves are therefore fundamental to clinical radiobiology.

A dose-response curve is a plot of biological response observed (e.g. tumor control, normal tissue injury) against the dose given. Both tumor control probability (TCP) and normal tissue complication probability (NTCP) increases with dose according to a sigmoid relationship as shown in Figure 2.4 below.

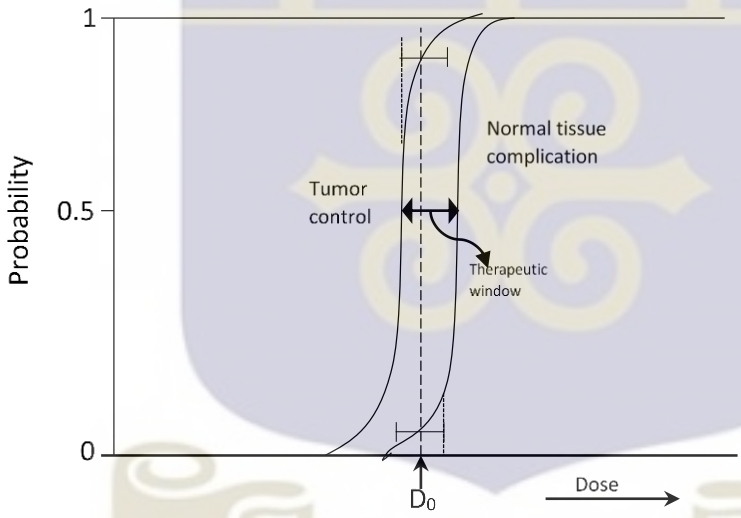

Figure 2.4: Tumor control and normal tissue complication probability against dose. D0 is the planned treatment dose and the vertical dashed lines indicate the change in response due to small changes in dose.

Tumors that may be successfully treated by radiotherapy are those in which the TCP curve lies to the left of the NTCP curve for the limiting normal tissues. So that the dose

required to achieve a high probability of tumor eradication is lower than that leads to significant normal tissue damage.

Figure 2.4 illustrates the ultimate goal of radiotherapy, which is to give the highest possible dose to the cancer bearing tissue to maximize the TCP and simultaneously minimizing the NTCP. The gap between the TCP and NTCP curves at the 50% response dose level (D_{50}) is known by "Therapeutic Window". The wider the therapeutic window is the easier to achieve the goal of radiotherapy. For tumor control the D_{50} value increases with tumor size [54] and for normal tissue morbidity it decreases with larger irradiated volumes [55]–[60]. This means that the therapeutic window narrows for large tumor sizes.

The figure also provides a diagrammatic illustration of the need for accuracy in dose delivery. Increasing the dose by even a small percentage above the dose D_0 would cause a significant increase in normal tissue damage, where as a decrease in dose would significantly reduce the probability of tumor control.

A parameter called normalized dose gradient γ [61] which is defined as the percentage increase in biological response for 1% increase in dose indicates the steepness of the dose-response curve. Values for γ calculated from actual clinical data vary from 1.5 to 7. This means that the error in dose delivery amplifies between 1.5 to 7 times when viewed as dose related part of the uncertainty in biological response. [22].

Several studies have formulated the accuracy in the delivery of absorbed dose to a patient during radiotherapy. Based on a review of the relative steepness of dose-response curves for local tumor control and normal tissue damage, a combined uncertainty of 5% [42],

3.5% [62], 3% [63] was proposed in dose delivery. Considering the complexity of the dose delivery process, it is difficult to achieve 3% or 3.5% accuracy in practice [64] and it is common to refer to the ICRU 24 [42] recommended accuracy level of 5% as the correction action level [22]. This is an overall uncertainty on the dose given to the patient at the end of all steps in dose delivery. It leads in turn to tighter accuracy requirements on each step in the radiotherapy process.

2.4.1 Sources of uncertainties in dose delivery

Table 2.1 summarizes sources of errors in dose delivery in to two groups, those that may arise during treatment phase and machine calibration and those that may be introduced during treatment preparation or treatment planning.

Table 2.1: Classification of sources of errors in external beam radiotherapy

Errors during patient treatment and machine calibration	Errors during treatment planning
Machine calibration	Patient data uncertainties
Monitor stability	Dose calculation
Beam Flatness	
Beam and patient set up	

Dose calculation errors could potentially affect the whole course of treatment and therefore are of particular concern. MU calculation (dose calculation) errors can be classified in to two broad types, random and systematic errors. A random error is not reproducible by its nature. It is mostly due to human mistakes and includes incorrect look

up of a table parameter (wrong energy, field size, SSD, depth, etc.), transcription errors, rounding of errors and so on. The other classification is systematic error. It is generally a result of a fault somewhere in the calculation procedure. Examples of systematic errors are errors in beam data, algorithmic error, etc.

For the calculation of MUs as part of a computerized treatment plan errors are mostly systematic, such as errors due to computer bugs, automatic data transmission, data corruption etc. Although the acceptance testing and commissioning procedures are designed to verify the accuracy and safety of beam data and algorithm used by TPSs, untested situations and errors during commissioning may also contribute to systematic errors [20]

Dose calculations errors may further be categorized into random and systematic errors. Random errors are not reproducible by nature, they can be avoided if the calculation is checked by another person. Using incorrect beam energy, wrong beam modifiers, mistakes in reading tables, wrong dose are all examples of random error. Systematic errors on the other hand are due to causes attributed to a fault somewhere in the calculation procedure [65]. Unlike random errors they may not be detected if the calculation is repeated by a different user. Examples of systematic errors are: an incorrect entry in the dosimetric data table used for calculation, an algorithmic error or misuse of the software used in dose calculations [20].

2.4.1 Accuracy requirements of dose calculation systems

A traditional approach for setting the tolerance level for dose calculation error alone is to identify other sources of uncertainties in the dose delivery chain and vary the dose

calculation error to recognize the limit where the overall value is severely affected by the dose calculation error [22]. The uncertainty in the determination of absorbed dose at the calibration point has been determined by [66]. Excluding monitoring instabilities, they have stated the absolute dosimetric uncertainty to be 2% for x-ray photon beams and 1.6% for Co-60. Combining these uncertainty estimate in dosimetry and estimate of uncertainties in the other steps of the dose delivery process from [63], Ahnjeso and Aspardakis [22] recommended that dose calculations need not be better than 2% (1SD) with a correction action level of 4%. This uncertainty estimates do not include uncertainties in geometry, it is only the dosimetric uncertainty [67].

2.5 Some previous accuracy verification studies on TPS calculated MUs for tangential breast irradiation

Several studies [4], [68], [69] have been done to evaluate the accuracy of the photon convolution/superposition dose calculation algorithm for computing dose under conditions simulating tangential breast irradiation. However, all of the studies were for the implementation of the algorithm on pinnacle treatment planning system. Baird et al [68] evaluated the accuracy of the algorithm with measurements made in breast phantom, fabricated from wax, using TLD and radiographic films for 6MV and 18MV photon beams. The calculated and measured doses agreed to within ±3% for both film and TLD measurements. In another study done by Howlett et al [69] for 4MV, 6MV, and 18MV X-rays, calculated point doses with the algorithm were compared with measured doses within an anthropomorphic phantom using ionization chamber and variation within a range of 0.8% to 4.5% were reported. Similarly Kirsner et al [4] has corroborated the

accuracy of MU calculation, performed by pinnacle TPS for intact breast irradiation with 6MV X-rays, with measurements made in a unique anthropomorphic phantom using ionization chamber. Average ratio (measured over calculated dose) 0.998±0.009 was obtained.

2.6 Some previous work on calculation of MU for tangential breast irradiation using 2D method

A number of methodologies for calculating MUs for tangential breast fields using a reduced field size to account for loss of full scatter conditions as a result of the flash and the curvature of the breast and chest wall have been reported. Prado *et al.*[8] have estimated the "effective field size" to accurately account for the amount of scatter present in the irradiated breast as area of a triangle. Their method resulted in a mean ratio of 1.013 ± 0.003 (3SD) between the effective triangle method MU calculation and 3D TPS calculation.

Prado *et al*. [8] compared MU calculations with and without heterogeneity corrections with the aim of assessing the importance of heterogeneity corrections in manual verification calculations. They found mean ratios of 1.006 (SD 0.016) and 0.992 (SD 0.008) for the ratios of uncorrected manual to TPS and heterogeneity corrected manual to TPS calculated MUs respectively. From the heterogeneity results that are presented in their work, they commented that heterogeneity corrections incorporated into dose calculation systems will not affect absolute dose delivery to any appreciable extent. Their data suggested that the most important factor influencing accuracy of dose calculations is perfect modelling of the reduction in scatter rather than explicit incorporation of heterogeneity corrections. Similarly Ellen *et al.*[70], Pierce *et al.*[71], and Kay Meyer

[10] all suggested correction methods to better account for surface shape and scattering characteristics in 2D MU calculations for breast tangents.

Kay and Dunscombe [9], with the aim of reconciling the disagreement between TPS calculated and manually calculated MUs for tangential breast fields, proposed to rearrange the breast tissue into a rectangular prism providing equivalent scatter to the calculation point. Estimation of the size of the rectangular prism was based on replacing the breast contour with a triangular or elliptical contour. The triangle approximation resulted in an average difference of -4.4% and standard deviation 1.4 % (1SD) and the elliptical approximation had an average difference of -1.2% with standard deviation of 1.7% (1SD) from the TPS calculation.

Although the methods discussed above and other similar methods [10] accounted for the loss of full scatter conditions for breast tangent to an extent that difference between the manual calculations and complex 3D algorithms was within 2%, they were based on estimations and assumptions. They did not consider regions of less scattering properties individually, rather they were based on randomly removing some portions of the irradiated volume up to the required level when agreement with TPS calculations is achieved. Whether the same scatter correction method can be applied for calculation of MUs for actual dose delivery is doubtful.

CHAPTER THREE

3. Materials and Methods

3.0 Introduction

The following chapter describes the Excel program developed to calculate MU for tangential breast irradiation, followed by the experimental method employed to test the accuracy of the MU calculations for tangential breast irradiation with the TPSs at SGMC and KBTH.

3.1 The Excel MU calculation program

The Excel program has two purposes. First for the calculation of monitor-units (MU) for 2D tangential breast plans at KBTH. Secondly, to be used as a second check for MU calculations performed as part of a 3D computerized treatment plans at KBTH (with Prowess Panther 3D TPS) and at SGMC (Oncentra 3D TPS).

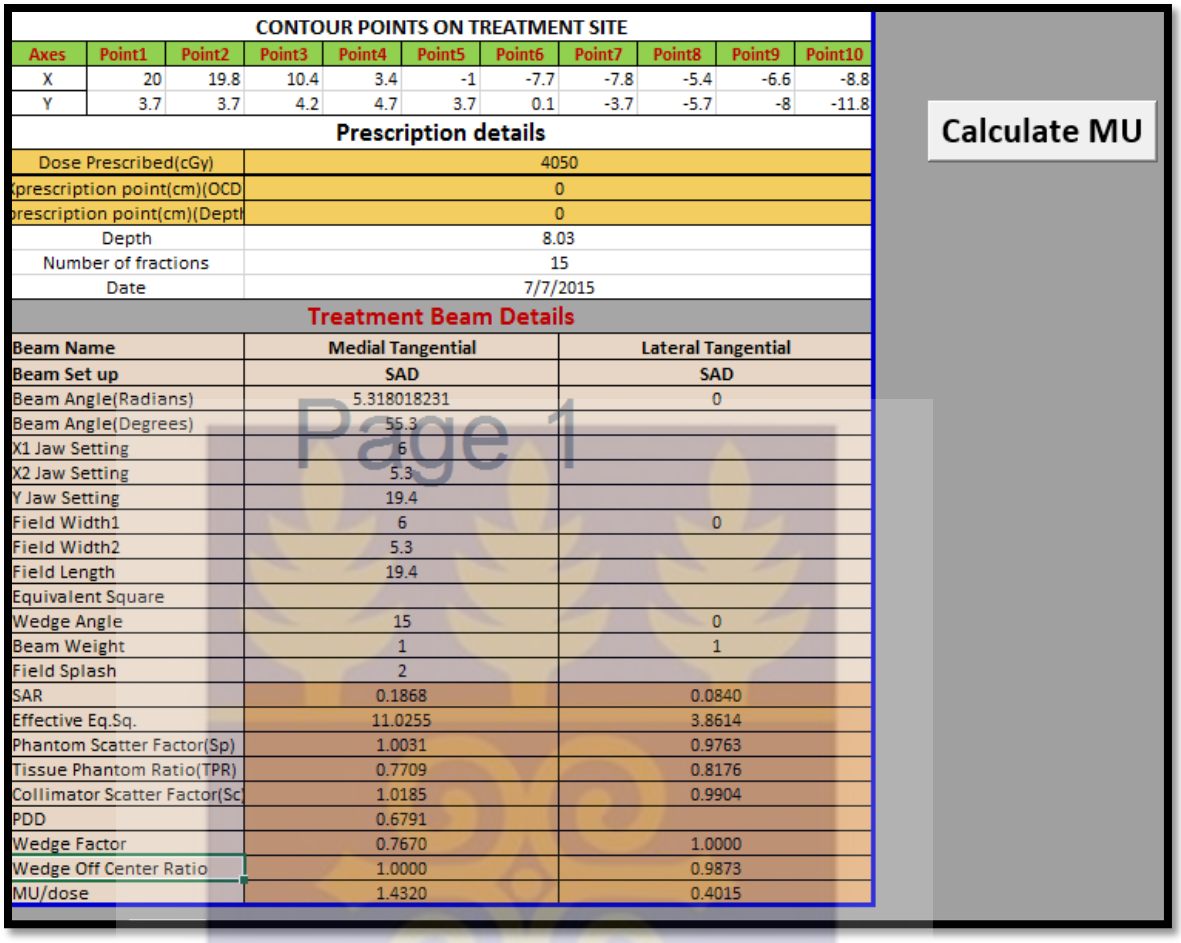

CONTOUR POINTS ON TREATMENT SITE

Axes	Point1	Point2	Point3	Point4	Point5	Point6	Point7	Point8	Point9	Point10
X	20	19.8	10.4	3.4	-1	-7.7	-7.8	-5.4	-6.6	-8.8
Y	3.7	3.7	4.2	4.7	3.7	0.1	-3.7	-5.7	-8	-11.8

Prescription details

Dose Prescribed(cGy)	4050
prescription point(cm)(OCD	0
prescription point(cm)(Depth	0
Depth	8.03
Number of fractions	15
Date	7/7/2015

Treatment Beam Details

Beam Name	Medial Tangential	Lateral Tangential
Beam Set up	SAD	SAD
Beam Angle(Radians)	5.318018231	0
Beam Angle(Degrees)	55.3	
X1 Jaw Setting	6	
X2 Jaw Setting	5.3	
Y Jaw Setting	19.4	
Field Width1	6	0
Field Width2	5.3	
Field Length	19.4	
Equivalent Square		
Wedge Angle	15	0
Beam Weight	1	1
Field Splash	2	
SAR	0.1868	0.0840
Effective Eq.Sq.	11.0255	3.8614
Phantom Scatter Factor(Sp)	1.0031	0.9763
Tissue Phantom Ratio(TPR)	0.7709	0.8176
Collimator Scatter Factor(Sc	1.0185	0.9904
PDD	0.6791	
Wedge Factor	0.7670	1.0000
Wedge Off Center Ratio	1.0000	0.9873
MU/dose	1.4320	0.4015

Calculate MU

Plate 3.1: User interface of the developed Excel MU calculation program

Improvements in the program from the manual MU calculation method that is currently being used for the above mentioned purposes at the two centers include, accounting for the irregular surface contour of the breast and off axis point calculations. The program was written in visual basic for applications (VBA) programming language in Microsoft Excel environment. The user interface for the Excel program is shown in Plate 3.1. It takes coordinates of points on a single transverse contour of the patient, irradiation parameters, dosimetric functions, and the prescribed dose as inputs. The flowchart of the program execution is shown in Figure 3.1.

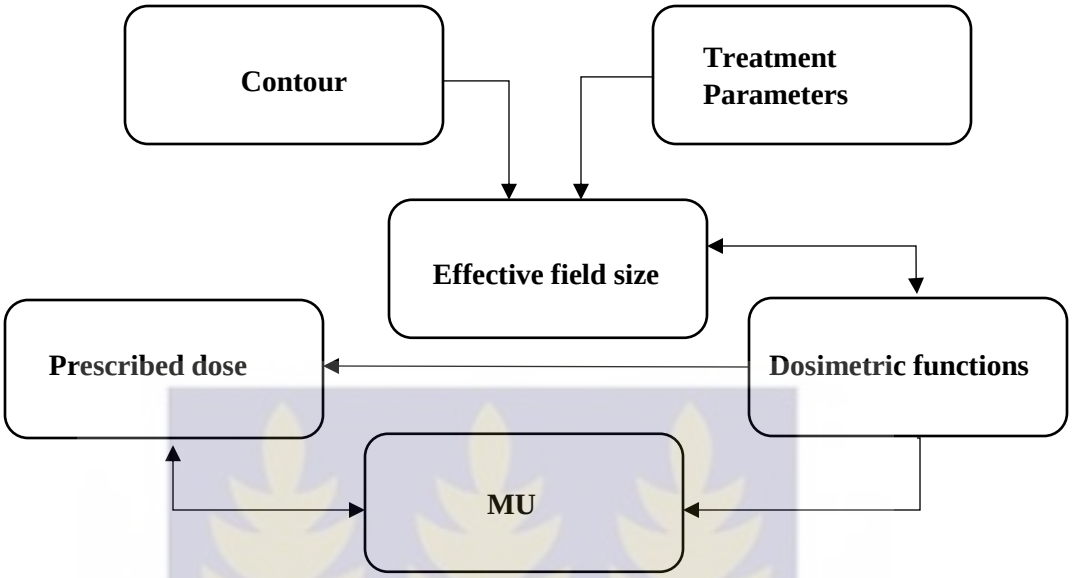

Figure 3.1: Flowchart utilized by the Excel MU calculation program.

For the proposed use of the program for the calculation of MUs for 2D treatment plans at KBTH, information on irradiation parameters and patient contour was obtained from the simulation chart from the simulation room. The chart contains a single transverse contour of the patient taken from the plane containing the central axis of the tangential beams, gantry angle and field size information. Marked on the contour curve are "off center" and "TLD" points to indicate where the sagittal and horizontal lasers, respectively, touch the transverse section of the patient where the contour is taken. On the chart a vertical (Y axis) line is drawn through the off axis point and a horizontal (X-axis) line is sketched through the TLD point. It should be noted that the point of intersection of the two lines is the location of the axis of rotation of the gantry at the transverse plane of the contour. Ten (10) points are marked on the contour and their X and Y coordinates are measured using a set square and entered into the program. Similarly the dose prescription point is also indicated on the outline curve and its coordinates are measured and entered.

For the intended use of the program for independent check of MUs calculated as part of 3D treatment planning at the two centers, data on the treatment parameters and the surface contour are extracted from the treatment plans with the TPSs. On the planning CT slice containing the MU calculation points, ten (10) calculation points are placed around the external contour where the tangential fields are. One (1) calculation point is also placed at the normalization (prescription) point. The coordinates of the calculation points with respect to the isocentre is then extracted from the TPS. For the Oncentra treatment planning system, measurement of the coordinates is relative to the center of the patient. The program performs translation operation on each calculation point to get the coordinates relative to the isocentre. From the Oncentra TPS it is also possible to obtain the radiological depth to the calculation point unlike the Prowess Panther which only displays the actual depth.

In order to calculate MUs for a given tangential radiation beam with gantry angle θ, the dose calculation method in this work requires the depth and off axis distances of points within the irradiated volume. Depth measurements should be made along a line parallel to the central axis of the beam and off axis distances of points should be measured along the width of the radiation beam. For this purpose the program multiplies the input coordinates of the contour points and the calculation point by the rotation matrix R given by:

$$R = \begin{bmatrix} \cos(\theta) & \sin(\theta) \\ -\sin(\theta) & \cos(\theta) \end{bmatrix} \qquad (3.1)$$

Where θ is the gantry angle.

This action is equivalent to rotating the original X and Y Cartesian coordinate system through the gantry angle θ about the axis of rotation of the gantry and measuring the coordinates of the points relative to the new coordinate system X′Y′. The transformed coordinates of the contour and calculation points will be referred to as X′ and Y′ to avoid confusion with the original X and Y coordinates. For dose calculations the transformed coordinates of the points were used. Figure 3.2 shows transformation of the original XY coordinate system, with respect to which coordinates of points on the patient contour is measured, into a new coordinate system X′Y′ that has its Y′ axis along the axis of the radiation beam and X′ axis parallel to the width of the radiation beam.

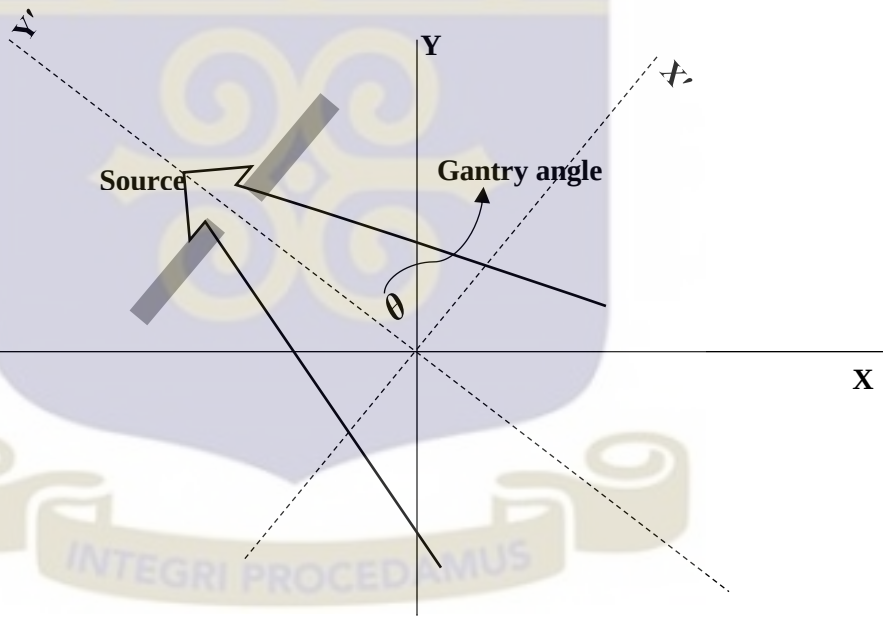

Figure 3.2: Transformation of the patient coordinate system to the beam coordinate system

3.1.1 Determination of depth of the calculation point

For the case of 2D treatment plans depth of the calculation point is obtained from the simulation procedure. For the 3D plans depth of the calculation point is retrieved from the TPSs. In Oncentra TPS it is possible to get the radiological depth of the calculation point while in Prowess the actual depth, the distance from the surface to the calculation point, can be obtained.

3.1.2 Determination of the effective equivalent square field size.

In the currently existing manual MU calculation methods at the two radiotherapy centers scattering conditions are accounted for by the dosimetric functions TMR and Sp. To read the values of these dosimetric values from look up tables the actual dimension of the field size given as adequate for tumor coverage is used. This might not give accurate results in the case of tangential breast irradiation, because in this case not the whole region of the radiation field is producing scatter to the calculation point as there is air splash and missing tissue around the irradiated breast or chest wall. To overcome this overestimation of scattered dose to the calculation point the differential scatter air ratio (dSAR) method of Cunningham [52] is implemented by the program. For the method SAR data obtained from Johns and Cunningham [31] was used for Co-60 beam at KBTH. For the 6MV and 15MV photon beams from the Elekta Linac at SGMC, SMR data were derived from Sp and TMR data using Khans [32] formula in equation (3.2) In what follows SMR data used for MU calculations for the LINAC also represents SAR for Co-60.

$$SMR(d,r) = TMR(d,r)\left(\frac{S_p(r)}{S_p(0)}\right) - TMR(d,0) \qquad (3.2)$$

Where $S_p(r)$ is phantom scatter factor for circular field size of radius r, S_p (0) is zero area phantom scatter factor extrapolated from S_p data for small field sizes, and TMR(d,0) is zero area TMR extrapolated from TMR data for small dimension fields.

The SMR data obtained were embedded into the Excel program in the form of tables. The X′Y′ contour curve is projected along the length of the radiation field to form a 3D contour surface. Clarkson's summation of SMR as a function of depth and radial distance from the calculation point is performed on the cross-section of the radiation field at the calculation point using the SMR data tabulated for circles. The depth to a point at a given radial distance is calculated as the summation of the Y′ coordinate of the point and the Y′ coordinate of a contour point that has the same X′ coordinate as the point (Figure 3.3).

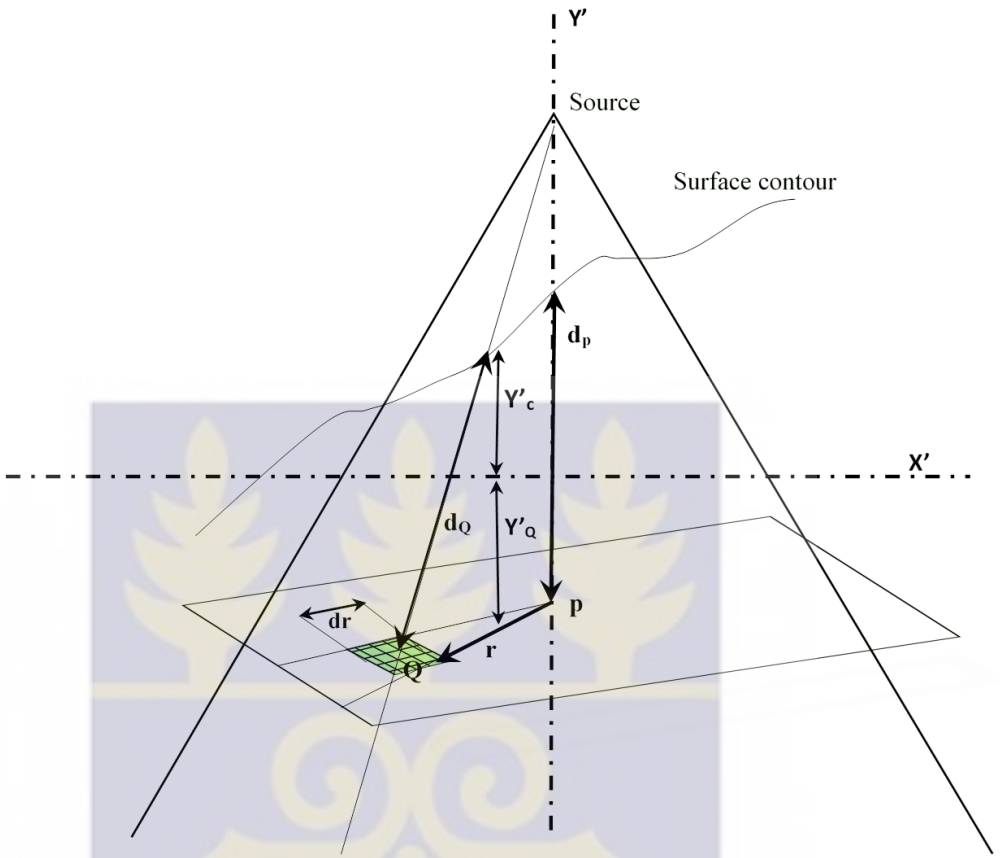

Figure 3.3: Diagram illustrating summation of SMR as a function of depth and radial distance from the calculation point p. The depth to point Q (d_Q) is the sum of the Y′ coordinate of the contour curve at point Q (Y'_c) and the Y′ coordinate of point Q (Y'_Q).

The cross section of the radiation field projected at the calculation point is subdivided into equal narrow sectors of central angle Δθ (5 degrees). Each sector is further divided into differential area elements of length Δr (0.0625cm) and width rΔr as shown in Figure3.3. Each sector is taken as a sector of a circle and the SMR for each differential area elements whose depth is taken variably according to the overlying contour surface is summed together as:

$$SMR = \sum_{i=1}^{n} \frac{\Delta\theta_i}{2\pi} \sum_{r=0}^{R} SMR(d_Q, r) - SMR(d_Q, r - \Delta r) \qquad (3.3)$$

The equivalent circle radius (R) that has the calculated total SMR at the depth of the calculation point is then looked up from the SMR data table. The effective equivalent square field size (E) is then calculated from the equivalent circles radius using equation (3.4) and taken as the effective equivalent square field size that will produce the actual scattered dose to the calculation point.

$$R = \frac{E}{\sqrt{\pi}} \qquad (3.4)$$

3.1.3 Dosimetric functions

Dosimetric functions are integrated in to the program in the form of Excel tables. Off axis ratio (OAR), collimator scatter factor (Sc), phantom scatter factor (Sp), percentage depth dose (PDD), wedge factors (WF), tissue maximum ratio (TMR), and scatter maximum ratio (SMR) data are extracted from the treatment planning systems used by the hospitals for 3D dose planning. OAR, Sc, Sp, PDD, and WF were measured and entered in to the TPSs during commissioning of the Equinox Co-60 unit (at KBTH) and Electa Synergy Linac (at SGMC). TMR and SMR data were derived by the TPSs from Sc, Sp and PDD data. In addition SAR data tables obtained from Johns and Cunningham [31] are incorporated into the software to determine the effective equivalent square field size as described above. TMR, PDD and Sp data were tabulated as a function of the effective equivalent square field size (E), depth (d) and wedge type (w). Sc data is tabulated in

terms of equivalent square field size (F) obtained by using the Sterling formula [46] in equation (3.5):

$$F = \frac{2 * W * L}{W + L} \qquad (3.5)$$

For the calculation of MU at off-axis points, the OAR was used to account for the effects of distances from the calculation point. The OAR was tabulated as a function of the equivalent square (F), depth, wedge type (w) and off-axis distance (x). Since the presence of wedge affects all the dosimetric functions, each dosimetric table was tabulated for open and wedged fields. For calculation of MUs for wedged and open fields, dosimetric functions obtained for wedged and open fields were used respectively.

Attenuation through the wedge filters is described in the MU calculation equation by the WF. KBTH mostly uses the external physical wedges for 2D planned treatments. The central wedge transmission factors are stored in a single Excel sheet for retrieval by the program.

The Linac at SGMC uses a single motorized (60^0) wedge. The central wedge transmission factor is incorporated into the collimator scatter factor Sp.

For all table look ups, when the given looking up parameter (field size, depth or off axis distance) is not tabulated linear interpolation technique is used by the program.

3.1.4 The MU calculation equation

For the Co-60 energy the MU required for a field to deliver the prescribed dose per field to the calculation point is calculated as:

$$MU = \frac{Prescribed\ dose\ per\ field}{\dot{D}_{com} \times TMR(E,d,w) \times S_p(E,w) \times S_c(F,w) \times WF(w) \times OAR(F,d,x,w) \times ISF \times f_{decay}} \quad (3.6)$$

Prescribed dose per field at the prescription point is:

$$Prescribed\ dose\ per\ field = \frac{Weight\ of\ the\ field}{Total\ field\ weights} \times \frac{Total\ prescribed\ dose}{Number\ of\ fields} \quad (3.7)$$

Where D_{com} is the reference dose rate of the Co-60 machine measured for reference conditions during commissioning of the machine, ISF is the inverse square factor to account for the calculation point being at the SAD distance as compared to the reference point of measurement for the reference dose rate which is at SAD+d_{max} distance from the source.

$$ISF = \left(\frac{SAD + d_{max}}{SAD}\right)^2 \quad (3.8)$$

The Equinox Co-60 machine at KBTH has a SAD of 100cm and the depth of maximum dose for Co-60 photon beams is 0.5cm. This makes ISF to be equal to 1.01.

f_{decay} is the decay factor to take into account for the decay of the source. The Program uses the date of commissioning and the current date from the computer to calculate the decay factor as:

$$f_{decay} = e^{\frac{-0.693 \times t}{5.27}} \quad (3.9)$$

Were t is the time difference (in years) between the date of commissioning and the current time and 5.27 is half-life of Co-60 source in years.

For SSD techniques PDD is used in place of TMR.

For checking the accuracy of the MU calculated by the Oncentra TPS at SGMC the program retrieves the calculated MU and the radiological depth to the calculation point and computes the dose delivered at the calculation point. Then the accuracy of the MU calculation will be checked indirectly by comparing the prescribed dose to the calculation point and the dose calculated with the program

Since the Linac machine has a single 60^0 wedge, smaller wedge angles are produced by delivering a given MU with and without wedge. The dose at the prescription point associated with the MU delivered without wedge is computed as:

$$Dose(Open) = Wedge\ out\ MU \times K \times TMR(E,d) \times S_p(E) \times S_c(F) \times ISF \times OAR(F,d,x) \quad (3.10)$$

Similarly the dose as a result of the MU given with wedge is:

$$Dose(W) = Wedge\ in\ MU \times K \times WTMR(E,d) \times WS_p(E) \times WS_c(F) \times ISF \times WOAR(F,d,x) \quad (3.11)$$

Were K is the output of the LINAC which is 1cGy/MU at d_{max} under reference conditions. It should be noted that the Open beam and Wedged beam dosimetric functions are used in equation (3.10) and equation (3.11) respectively.

The total dose at the calculation point is then computed by adding the doses from equation (3.10) and (3.11)

3.1.5 Some assumptions and approximations made in the program as sources of uncertainties in using the program (Limitations of the program).

The program, to determine depths of scattering elements for the purpose of scatter calculations, uses coordinates of points on the surface of the breast or chest wall region where the radiation enters. The program constructs the surface of the breast from a single transverse contour taken assuming that the curvature of the breast or chest wall is uniform

over the whole transverse segments. The constructed surface contour might differ significantly from the actual skin shape and lead to calculation error for very irregular breast or chest wall surfaces.

For cases of irradiation with Linac beams the program uses SMR data derived from zero area TMR data which is also derived by linear extrapolation from TMR data for 4 X 4 cm^2 and 5 X 5 cm^2. Since TMR is a very nonlinear function of field size for smaller field dimensions, linear extrapolation to zero field size might be very uncertain.

3.2 Verification of the accuracy of MU calculations with Prowess Panther and Oncentra Treatment planning systems for irradiation of the breast with tangential fields.

In order to test the performance of the Excel program, its outputs were compared with the respective outputs from Prowess Panther and Oncentra treatment planning systems. However, there was no guarantee that the TPS-calculated MUs are accurate enough as with some algorithms it may be difficult to model a particular clinical setup [50]. Therefore accuracy of the MU calculation results of the TPSs was first validated with measurements made in anthropomorphic phantom using calibrated Gafchromic EBT2 films.

Next the materials and methods employed to verify the TPS calculations using the calibrated films will be presented.

3.2.1 Materials

The following materials were used in this work to validate the accuracy of MU calculations with Prowess Panther and Oncentra treatment planning systems:

- Theratron Equinox 100 cobalt-60 teletherapy unit
- Elekta synergy linear accelerator
- Varian Equity treatment simulator
- Prowess Panther Treatment Planning System version 4.6
- Oncentra Treatment Planning System version 4.3
- EPSON scanner
- Gafchromic EBT2 film
- Siemens CT scanner (single slice)
- Siemens Emotion duo CT scanner (16 slice)
- I view GT imaging system
- Plastic phantoms
- Alderson Rando anthropomorphic phantom
- Image J software version 1.48
- Microsoft Excel 2013

3.2.2 Calibration of EBT2 Gafchromic films

Before the use of films for absolute dose measurement the film needed to be calibrated first with a known dose. The method used to calibrate Gafchromic EBT2 films was as follows:

Along the long end of a new Gafchromic EBT2 film, a strip of length 1.5cm was cut using a pair of scissors. The strip was then divided into pieces of width 2 cm, making each piece 1.5 cm × 2 cm. This way of cutting the film helps to preserve orientation of the original film as dosimetry with radio chromic films is affected by film orientation [34]. One of the pieces was then placed on a pile of plastic phantoms under Elekta Linac unit at the center of an open 10 cm × 10 cm field at 100 cm distance from the X-ray source as shown in Plate 3.2 below.

Plate 3.2: A piece of Gafchromic EBT2 film placed on a pile of plastic phantoms at the center of a 10 cm × 10 cm 6MV radiation field from Elekta Linac.

The pile of plastic phantoms was to produce full scatter conditions. Another pile having a water equivalent thickness of 5cm was placed on top to make the film at 5cm water depth. MU required to deliver 50cGy with 6MV X-rays to the film was calculated. Three

(3) separate films were irradiated to the calculated MU so as to average out variations within the film. Similarly films were irradiated from 100cGy up to 350 cGy in 50cGy intervals.

After 18 hours of storage in dry and dark location, the films were scanned using Epson flatbed scanner. The scanner is a 16 bit RGB scanner and has only reflection mode of scanning. Prior to the scanning the color correction option of the scanner was turned off as it alters the pixel values. The films were scanned in landscape orientation in order to reduce variations within the film, as recommended by the manufacturer. To factor out variations with scans as a result of warm up of the scanner each film was scanned three times.

Image J software was used to read the pixel values of the scanned images of the irradiated films. The pixel value is a measure of the amount of light that is transmitted through the film during scanning. Optical density can be calculated from transmission (T) using the relation:

$$OD = \log\left(\frac{1}{T}\right) \tag{3.12}$$

It is the optical density that has a direct relationship with dose, however the transmission or the pixel values were used. Since the same scanner was used for scanning the calibration films and the films for dose measurements the conversion of transmission into density was not necessary.

EBT2 films have their greatest response in the red color channel [37]. Therefore reading of the pixel values were made in the red color channel.

Since the films were irradiated three times for each dose level and scanned three times, the pixel value for each dose level was averaged. The resulting pixel values and the corresponding dose values were entered into the calibration function of Image J. Exponential function is used for fitting the calibration curve as shown in Figure 4.1 in the Results.

3.2.3 Verification of accuracy of Prowess Panther TPS for calculation of MUs for tangential irradiation geometries

Alderson Rando anthropomorphic phantom was used for the verification (Plate 3.3). It has removable breasts and can be dismantled into transverse segments for the placement of detectors. The verification was done for two plans: one for the left side with the breast removed to represent chest wall irradiation after mastectomy and one for the right side with the breast attached to represent intact breast irradiation.

Plate 3.3: Alderson Rando anthropomorphic phantom with removable breasts

First, both the chest wall and intact breast irradiations were simulated on Varian conventional simulator and field borders were drawn on the surface of the phantom. After the simulation, the phantom was disassembled and eight (8) tiny lead markers were cut and placed at selected points under one of the slices between the inferior and superior field borders; four (4) for the chest wall irradiation and four (4) for the intact breast irradiation. Medical tapes were used to hold the lead markers in place and numbers were written on them to identify the lead points (Plate 3.4). The points at which the lead markers were placed were chosen to be far enough from the edges of the phantom to make sure that the points are not within high dose gradient areas such as dose build up and penumbra regions.

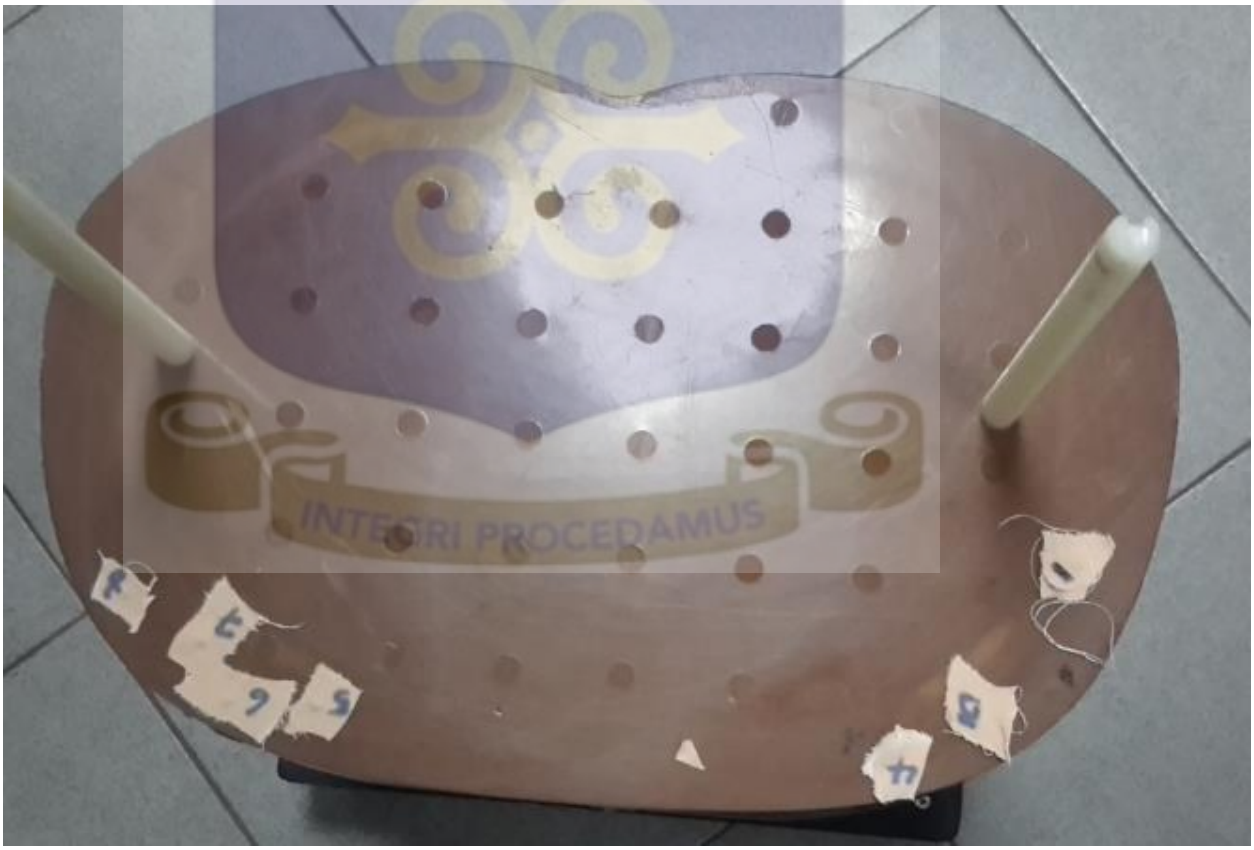

Plate 3.4: Tiny lead marks placed in one of the slices of the phantom. The numbers on the medical plaster used to secure the leads in place identify the lead points.

The phantom was then assembled and CT scanned on a diagnostic CT scanner (Siemens single slice CT scanner) with flat table top. The lead marks appeared as small bright spots on one of the CT slices and produced streak artifacts on two of the adjacent CT slices (Plate 3.5).

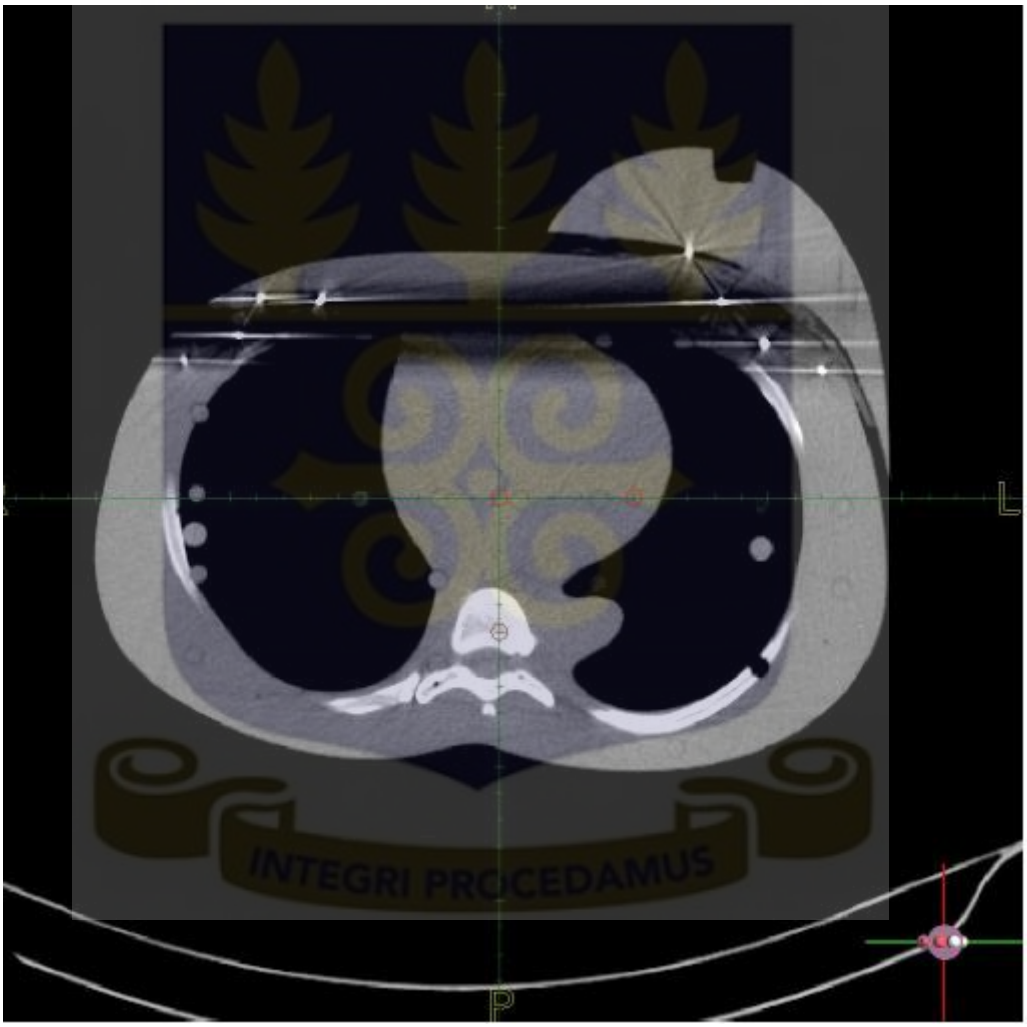

Plate 3.5: CT slice image of the anthropomorphic phantom showing the lead markers and the streak artifacts they produced.

The CT image was imported into the TPS for dose planning. Calculation points were placed on each of the images of the lead marks. As shown in Plate 3.6, calculation points were numbered according to the numbering of the lead points. Calculation point 1 was placed on lead mark 1 calculation point 2 on lead mark 2…. etc. The streak artifacts were corrected by the artifact correction tool of the TPS. The artifacts appeared as dark regions on three of the CT slices. Gray color that represents Hounsfield Unit value of 0 (for water) was painted all over the artifact region. During the process of correcting the streak artifacts calculation point 1 placed on lead point 1 was mistakenly displaced to other slices. Calculation points 2 through 7 were used for further analysis.

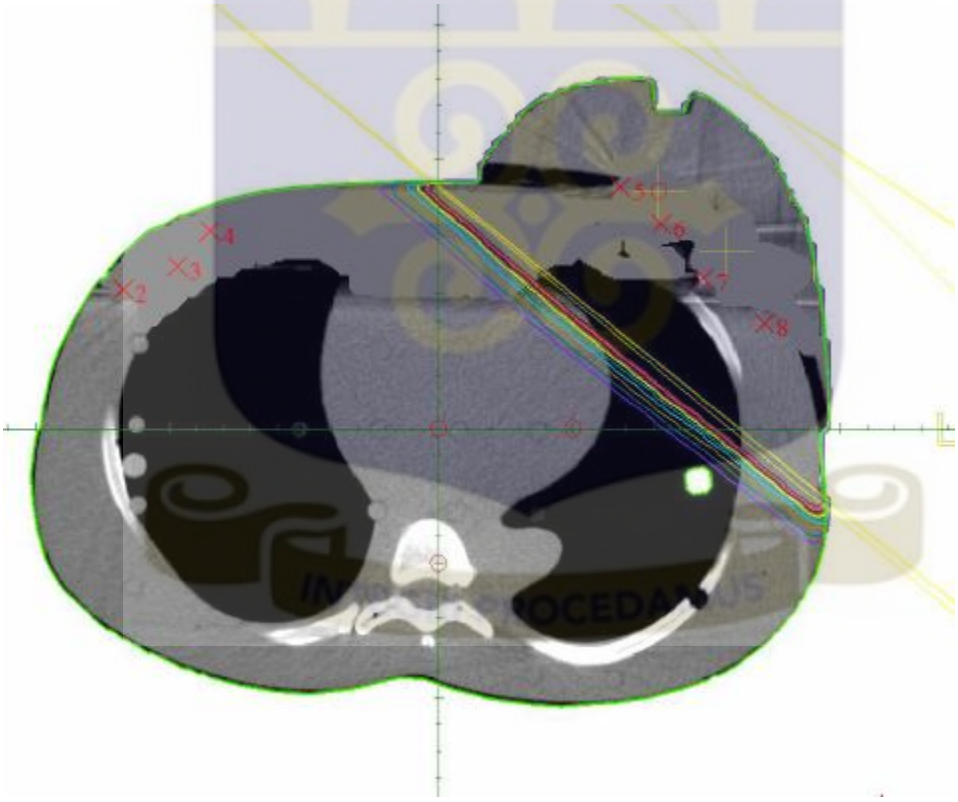

Plate 3.6: CT slice image of anthropomorphic phantom after the streak artifacts were corrected. Calculation points (red crosses) were placed on the images of the leads markers.

Two treatment plans were produced, one for chest wall irradiation and one for the intact breast irradiation, as per the centre's protocol for chest wall and intact breast irradiation. Two tangential beams (medial tangential and lateral tangential) were used for both plans. Two (2) Gy was prescribed at the isocentre for each plan. The resulting treatment chart containing the treatment parameters and point dose information table containing the coordinates and doses to the 7 calculation points was generated and printed.

In the treatment room the phantom was dismantled and the four lead marks on the left side of the breast were substituted with 1.5 cm × 2 cm rectangular pieces of EBT2 films (Plate 3.7)

Plate 3.7: Replacement of lead markers on the left side of the phantom with Gafchromic film pieces.

The phantom was assembled back and irradiated according to the treatment plan for the chest wall. The phantom was dismantled again and the irradiated four (4) film pieces were removed and placed in slots marked with numbers that indicated which calculation point the film represented. Similarly the remaining four (4) lead points on the right side of the phantom were replaced with film pieces and the phantom was irradiated according

to the treatment plan for the intact breast. After irradiation the films were removed from the phantom and were placed in dark location to be evaluated later.

After 18 hours the irradiated films were scanned with the Epson scanner in a similar way as the calibration films and the image was opened and analyzed with Image J software. The resulting pixel values were converted into dose value using the calibration curve produced in this study.

3.2.4 Verification of the accuracy of point dose calculation with Oncentra TPS

The same procedure was used to validate the point dose calculation of Oncentra treatment planning system used at SGMC. The difference was that Siemens 16 slice CT scanner was used and due to the protocol at SGMC, the phantom had to be irradiated with the films inside for an additional small number of MUs to verify that the position of the phantom on the treatment couch was exactly as it was planned in the TPS. This was done by superimposing and matching the digitally reconstructed radiographs (DRRs) and the online image produced by the electronic portal imaging device (EPID) using the iView GT imaging system. When the verification was performed for the chest wall plan the positioning was found to be perfectly the same as the planned position. For this reason irradiation of the intact breast plan was performed without verification.

Another difference was that both the intact breast and chest wall irradiations were made on the right side of the phantom. After irradiation of the chest wall (with the right side breast removed), the breast was attached for the intact breast irradiation.

3.2.5 Verification of the Excel Program with Prowess Panther and Oncentra TPSs

The accuracy of the excel programme discussed in section 3.1 was verified by comparing its computation outcomes with those from Prowess Panther and Oncentra planning systems.

From the database of Prowess Panther TPS all 3D breast plans of women cancer patients were retrieved. They were nine in number (five intact breasts (two right and three left) and four chest walls after mastectomy (three right and one left). Seven of the cases were irradiated with wedged parallel opposed Co-60 beams and two of them were irradiated with open beams.

Each plan was opened and on the planning CT slice containing the normalization point, ten (10) calculation points were placed around the external surface curvature of the irradiated area and a single calculation point was placed on the normalization point (Plate 3.8).

The origin of the coordinate system of the planning window with respect to which coordinates of calculation points is specified was placed at the isocentre. The XY coordinates of the calculation points were generated using the "calculation points summary" function of the TPS and transcribed in to the Excel programme.

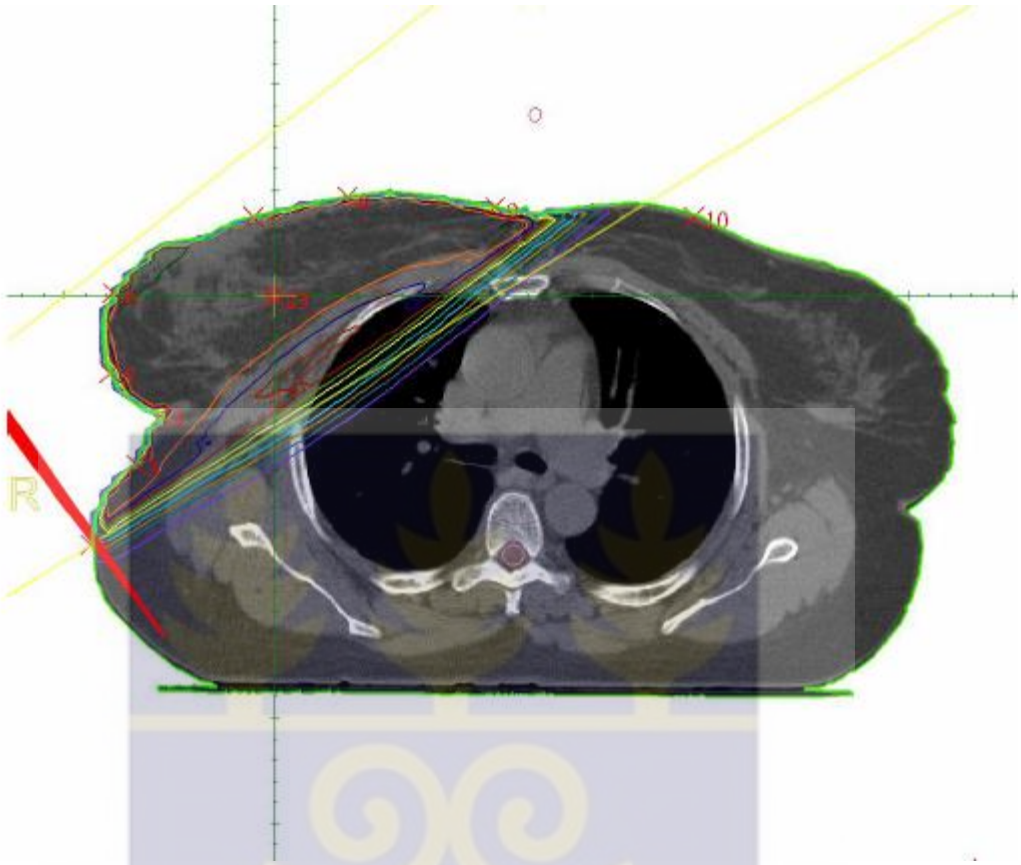

Plate 3.8: Extraction of contour information from the CT slice containing the normalization point.

The planned treatment parameters including gantry angles, prescribed dose to the normalization point, beam weighting, and field sizes were all extracted from the 3D plan using the " photon plan summary" tool of the TPS and transferred in to the Excel programme. The excel programme is executed and the calculated treatment time based on the entered contour information and treatment parameters is compared with the treatment time computed with the TPS.

From the Oncentra TPS a total of thirteen (13) 3D plans for irradiation of intact breast or chest wall with 6MV and/or 15MV tangential X-ray beams were retrieved. The same procedure used for Prowess Panther was used to extract contour information and the

planned treatment parameters. Except, in the case of Oncentra instead of the prescribed dose to the normalization point, the number of MUs required to deliver the prescribed dose to the calculation point with wedge and without wedge was retrieved. The Excel programme then uses the information to recalculate the dose to the normalization point and this was compared with the prescribed one.

3.2.6 Uncertainties in verifying accuracy of the TPSs due to limitations of the method used

The main aim of comparing TPS calculated doses with their measured counterparts was to assess the magnitude of error introduced in dose delivery, during tangential breast irradiation, owing only to drawback of dose computation with the TPSs. However, the observed deviations between the computed and measured doses could also be due to other sources of errors as the method used had limitations to exclude or quantify errors from another possible sources. The error due to difference between planned and actual irradiation geometries was not determined to be subtracted from the deviation measured. The uncertainty associated with measurements made with radio chromic films (relative dosimeter), which could be differentiated with parallel measurements made with ionization chambers (absolute dosimeter), couldn't be known due to the structure of the phantom used that has no room for ionization chamber. The inevitable statistical errors in measuring the doses could have been reduced to very minimum values. The two radiotherapy centers, however, were very busy and it was only possible to make a single measurement for a particular plan.

CHAPTER FOUR

4. Results and Discussion

4.0 Introduction

This chapter presents the results of the analysis of the outcomes of the experiments described in chapter three and discusses their implications. Analysis of the outcomes of the film calibration procedure performed to obtain the relationship between film gray values and absorbed dose will be addressed. The outcomes of comparison of calculated (with TPSs) and measured point doses will be given. Finally the comparison of MUs (or point doses) computed with the TPSs and the Excel program will be discussed.

4.1 Verification of accuracy of point dose calculations with TPS

4.1.1 Calibration of EBT2 Gafchromic film

The dose values for which the calibration films were irradiated and the corresponding pixel values (Gray values) were fed to the calibration function of the Image J software. The resulting curve (calibration curve) that relates the independent variable (pixel value) to the dependent variable (absorbed dose) is shown in Figure 4.1. An exponential function was fitted since it was the best fit based on the R^2 value. It can be seen from the curve that all the data points follow the trend of the curve and so the calibration curve was taken as acceptable for use in further analysis.

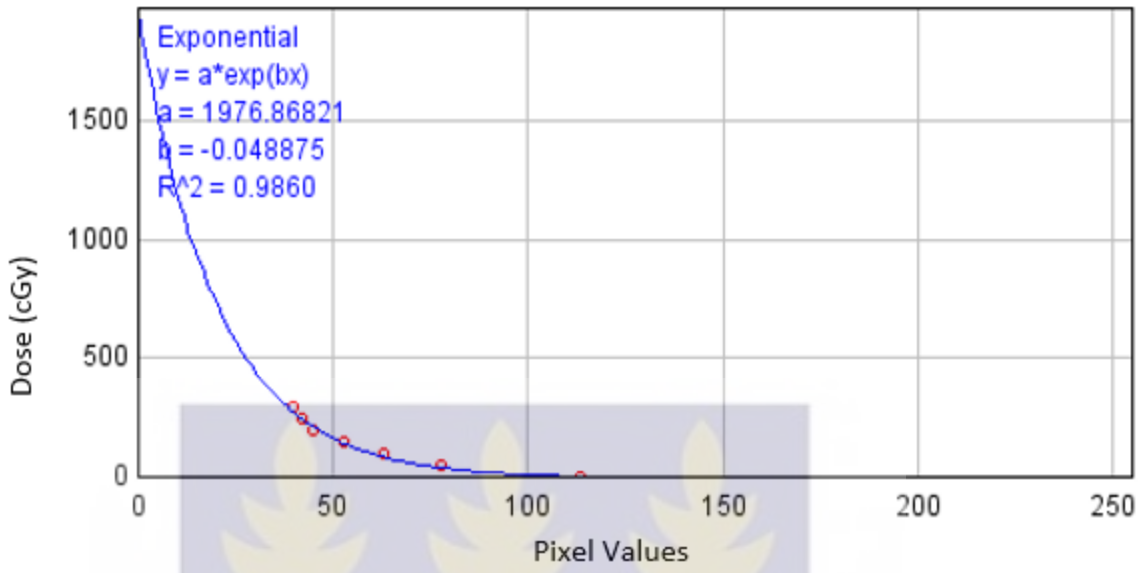

Figure 4.1 Calibration curve obtained by fitting exponential function to seven data points. The resulting exponential equation that relates pixel values (x) to absorbed dose (y) and the R2 value of the fitting is also shown.

4.1.2 Verification of point dose calculations with Prowess Panther and Oncentra TPSs

Table 4.1 and Table 4.2 respectively show the results of the comparison of point dose calculations with Prowess Panther and Oncentra TPSs and measurements made in calibrated anthropomorphic phantom with radiochromic film pieces. The percentage deviations between the measured and calculated doses were determined using equation (4.1) below.

$$\%div = \frac{D_{calc} - D_{meas}}{D_{meas}} \times 100\% \qquad (4.1)$$

The measured doses were used as the standard because it was the accuracy of the TPSs being verified.

Table 4.1: Summary of comparison of Prowess Panther TPS calculated point doses with measured point doses for irradiation of intact breast and chest wall with tangential Co-60 beams.

Chest wall			
Calculation point	Measured dose	Calculated dose	% deviation
2	215	211	-1.86
3	208	205	-1.44
4	215	213	-0.93
Intact breast			
Calculation point	Measured dose	Calculated dose	% deviation
5	201	211	-4.74
6	202	205	-1.46
7	208	199	4.52
8	197	204	-3.43

The deviation between the measured and calculated point doses with Prowess Panther TPS were within the range of -1.86% and -0.93% (mean of -1.41 and standard deviation of 0.38) for chest wall and -4.74% and 4.52 (mean of -1.28 and standard deviation of 3.55) for intact breast. The relatively high margin of error and standard deviation for the case of intact breast irradiation might be due to the presence of air gap between the chest wall and the breast of the anthropomorphic phantom as they were not matching perfectly during experimentation with the TPS at KBTH.

The measured and Oncentra TPS computed point doses had a percentage deviation within the range -4.42% to -1.55% (mean of -2.09 and standard deviation of 2.38) for chest wall and -4.04% to 3.14% (mean of -0.98 and standard deviation of 2.45) for intact breast irradiation. There was a relatively higher standard deviation for the chest wall case. It was suspected that the extra small number of MUs delivered to verify the setup of the phantom during irradiation of the chest wall of the phantom at SGMC is the cause for the higher standard deviation.

Table 4.2. Summary of comparison of Oncentra TPS calculated point doses with measured point doses for irradiation of intact breast and chest wall with tangential 15MV and 6MV X-rays.

Chest wall irradiation with 15MV X-rays			
Calculation point	Measured dose	Calculated dose	% deviation
1	193	190	-1.58
2	173	181	-4.42
3	191	194	-1.55
4	170	177	-3.95
Intact breast irradiation with 6MV and 15MV X-rays			
Calculation point	Measured dose	Calculated dose	% deviation
1	190	198	-4.04
2	194	194	0
3	195	200	-2.5
4	194	197	-1.52
5	197	191	3.14

It should be noted that the difference between the measured and computed point doses was not only due to limitations of the TPSs in beam modelling. Set up errors as well as film handling and uncertainties in reading of the films may have also contributed to the observed variations.

The point doses calculated by Oncentra TPS showed relatively better agreement with the measured ones. This could be due to the different setup verification protocols used by the two centres using the respective TPSs. At SGMC, verification of setup was performed by superimposition and matching of online images from the electronic portal imaging device (EPID) and DRRs, using a special software (iView GT imaging system), which is more accurate than the one used at KBTH, that is verification of the setup by side-by-side comparison of simulator radiographs and DRRs.

The results of verification of the point doses computed by the TPSs generally showed that the superposition-convolution dose calculation algorithm as implemented by Prowess Panther and Oncentra TPSs for point dose calculation of tangential breast fields is within ± 5% (including setup and dosimetric errors) of the measured doses. This gave a high degree of confidence in using the TPSs for further verification of MU calculations with the Excel MU calculation program.

4.2 Verification of the Excel MU calculation program.

The results of comparison of the outputs of the Excel program with those of Prowess Panther and Oncentra treatment planning systems is presented in Figures 4.2, 4.3 and 4.4 below. The percentage deviations between the outputs from the Excel program and those from the TPSs was calculated using the equation:

$$\% \, dev = \frac{R_{Excel} - R_{TPS}}{R_{TPS}} \times 100\% \qquad (4.2)$$

Where R_{Excel} is computation results of the Excel program and it can be MU or dose calculated at the MU calculation point. R_{TPS} is the corresponding computation result of the TPS. R_{TPS} is taken as the standard because the accuracy of the Excel programme is verified with the TPS.

Figure 4.2 shows the observed percentage deviations between MUs calculated with the Excel programme and Prowess Panther TPS. The deviations were within the range of -1.56% and 3.62% with a mean of 2.06% and standard deviation of 1.43.

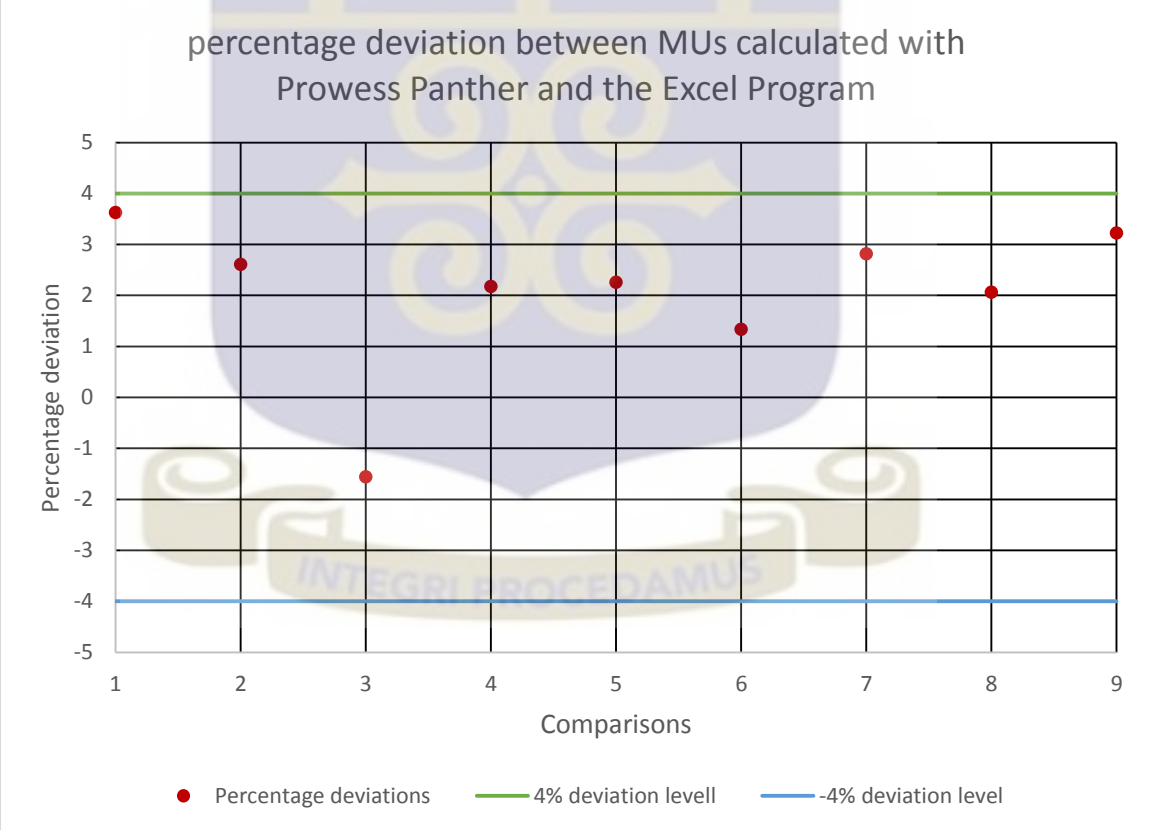

Figure 4.2. A chart depicting the agreement between MU calculations with Prowess Panther TPS and the Excel program. The upper and lower horizontal lines show the 4% and -4% deviation levels.

Percentage deviations between absolute dose computed with the Excel programme and Oncentra TPS for irradiation of the breast with 6 MV and 15 MV X-rays is diagrammatically represented in Figure 4.3 and Figure 4.4 respectively. In the case of 6MV the deviation had a minimum value of -2.60%, a maximum value of 3.70 %, a mean of 0.33% and a standard deviation of 2.59. The variation, for the case of 15MV, was in the range of -3.44% and 2.04% (mean of -0.31 and standard deviation of 2.02).

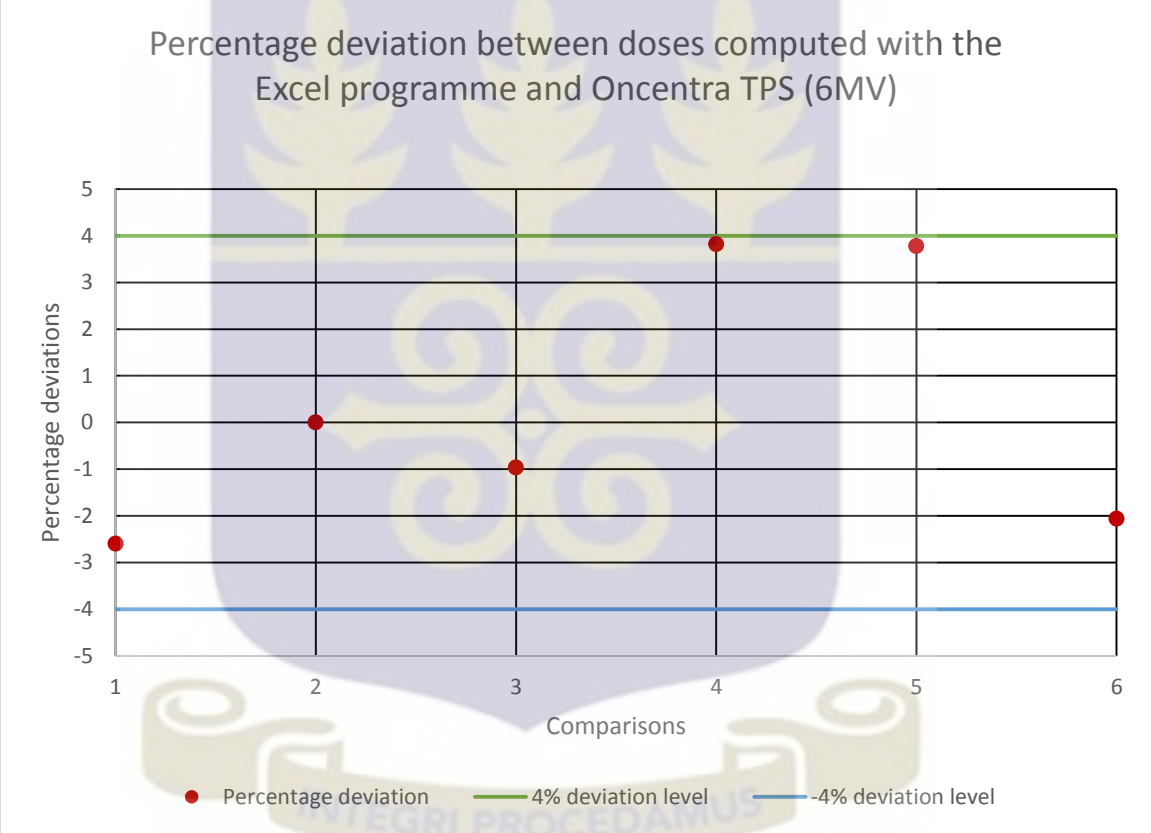

Figure 4.3: Percentage deviation of dose calculated with Oncentra and dose calculated with the Excel program for 6MV x-rays. The 6 markers are the percentage deviations of doses calculated for 6 plans.

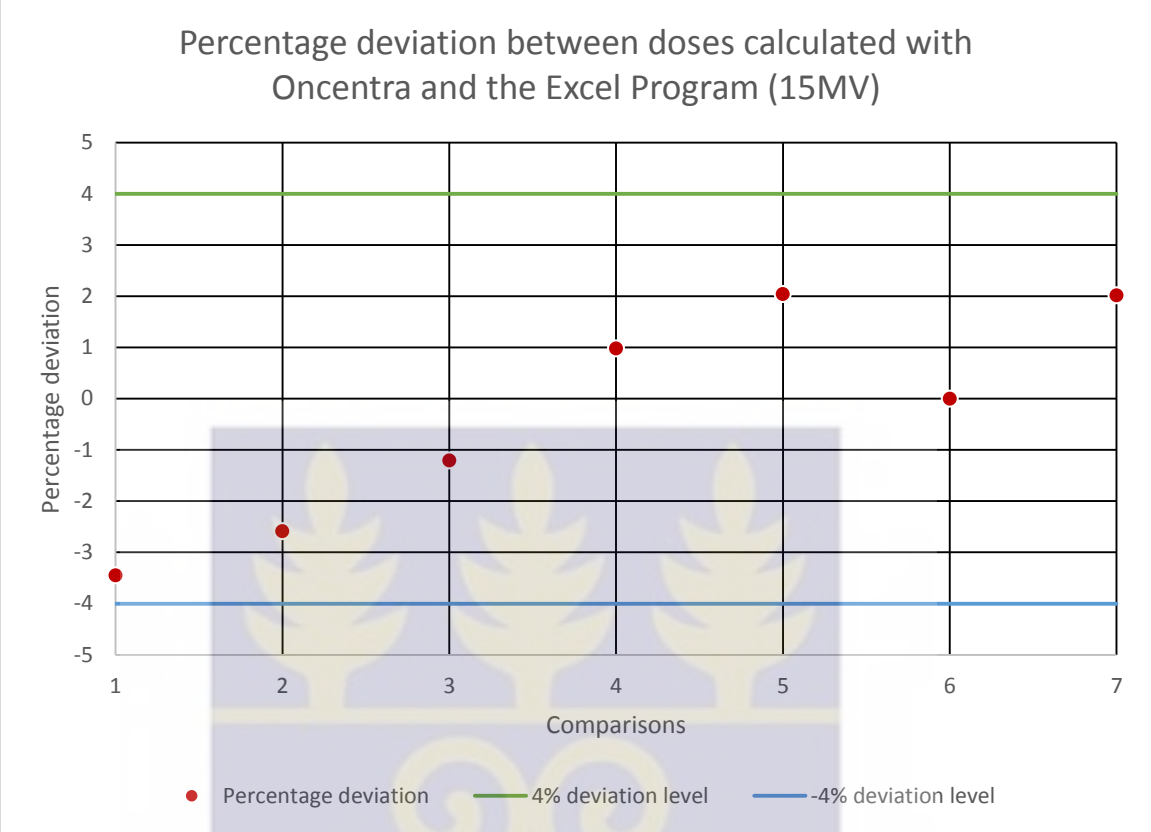

Figure 4.4: Percentage deviation of doses calculated with Oncentra and the Excel program for 15MV x-rays. The 7 markers are the dose ratio calculated for 7 plans.

The observed degree of deviations between the calculation results of the Excel program and the two TPSs is possibly due to the fact that computation with the Excel programme is based on a single contour information without inhomogeneity corrections whereas the TPSs can handle 3D inhomogeneity and scatter calculations.

TG-114 [20] specified an action level for the discrepancy between MUs calculated with a TPS and another method using different computation algorithm and approximate patient geometry to be ±4%, when the other MU calculation method is used to verify accuracy of the TPS calculations. All of the observed disagreements between the Excel programme and the 3D TPSs were within this ± 4% action level.

CHAPTER FIVE

5. Conclusion and Recommendations

In this work an Excel program for the calculation of monitor unit (MU) for tangential breast irradiation using a single transverse patient contour to account for loss of full scatter conditions has been developed. The contour information together with treatment parameters and dosimetric functions were used to calculate the effective equivalent square field size that will produce actual scattered dose at the calculation point employing Clarkson's summation of differential SAR/SMR in two dimensions.

Point dose computation results of Prowess Panther and Oncentra treatment planning systems for 3D tangential breast irradiation plans were compared with measurements made in anthropomorphic phantom using calibrated radiochromic films to test the accuracy of MU calculation with the TPSs. The TPSs were then used to test the accuracy of the Excel program.

The measured and calculated point doses had a percentage deviation ranging from -4.74% to 4.52% (mean of -1.33% and standard deviation of 2.69) for Prowess Panther TPS and from -4.42 to 3.14 (mean of -1.47% and standard deviation of -3.95) for the Oncentra TPS. In addition to the limitations of the TPSs, the observed deviation between the measured and calculated point doses is possibly due to uncertainties in phantom setup during irradiation and inaccuracies of the radiochromic film measurement.

The percentage deviation between MUs calculated with the two TPSs and the Excel program were within the range of -3.45% and 3.82% (mean of 0.83% and standard deviation of 2.25). The observed percentage deviations are within the 4% action level

recommended by TG-114. This indicates that the Excel program can be confidently employed for calculation of MUs for 2D planned tangential breast irradiations or to independently verify MUs calculated with TPSs as part of a 3D computerized treatment plan.

5.1 Recommendations for SGMC and the radiotherapy center of KBTH

1. The radiotherapy center of KBTH should validate MU calculations, regardless of the method of computation, with a second method that is independent from the primary MU calculation method.

2. Both centers should have reasonable action levels for the deviation between primary and verification MU calculations in order for the verification calculation to be effective in detecting treatment planning or dose calculation errors. It is preferable to use AAPMs TG-114 guide lines for action levels

3. At the radiotherapy center of KBTH, for calculation of treatment time for 2D planned tangential breast plans, a calculation method with scatter calculation capability should be employed. It is preferable to use the TPS with the 2D breast contour digitized in to it; however calculation methods that are employed in the developed EXCEL program could also be used.

4. SGMC should incorporate scatter corrections into the existing secondary MU calculation method for tangential breast irradiation with photon beams, in order for the outputs of the calculations routinely agree with the TPS calculations within reasonable deviations. The calculation method in the EXCEL program developed in this work could be employed.

5. KBTH and SGMC should validate the accuracy of the dose calculation algorithms as implemented in their respective TPSs for irradiation conditions that deviate significantly from commissioning irradiation geometries. The method used in this work could be adapted for the different irradiation conditions.

5.2 Other recommendations established from this research for future work

- For a better agreement with TPS calculated MUs, scatter computation methods in verification MU calculations for tangential breast irradiation, it is advantageous to:

    1) Incorporate functions to account for variation of scatter contribution to the calculation point with distance between scattering element and the calculation point as well as when the scattering element is vertically under different thicknesses of a wedge filter.

    2) Use SMR data derived from other accurate methods, such as through Monte Carlo simulation, than extrapolated zero area TMR data.

    3) Employ two or more transverse contours for very irregular breast or chest wall topographies

- For improved investigation of the magnitude of error that would be introduced into dose delivery, during tangential breast irradiation with external photon beams, due to limitations of the dose computation capabilities of TPSs alone, exclusive of errors from other sources

    1) The magnitude of setup error should be quantified first

2) Measurement of dose with radio chromic films for a given dose plan should be made multiple times in order to minimize statistical errors

3) In order to differentiate between errors measurement of doses with radiochromic films should be ascertained with measurements made with ionization chambers. For this purpose anthropomorphic phantoms that allow insertion of ionization chambers are preferable.

REFERENCES

[1] World Health Organization, "GLOBOCAN 2012: Estimated cancer incidence, mortality and prevalence world wide in 2012." [Online]. Available: globocan.iarc.fr/Default.aspx.

[2] C. Edward, Halperin, W. Luther, Brady, A. Carlos, Perez, E. David, and Wazer, *Perez & Brady's Principles and Practice of Radiation Oncology*, Sixth. Lippincott Williams&Wilkins, 2013.

[3] G. P. Delaney, S. Jacob, C. Featherstone, and M. B. Barton, "The role of radiotherapy in cancer treatment: Estimating optimal utilization from a review of evidence-based clinical guidelines," *Cancer*, vol. 104, pp. 1129–1137, 2005.

[4] S. M. Kirsner, K. L. Prado, R. C. Tailor, and J. a Bencomo, "Verification of the accuracy of 3D calculations of breast dose during tangential irradiation: measurements in a breast phantom.," *J. Appl. Clin. Med. Phys.*, vol. 2, no. 3, pp. 149–56, Jan. 2001.

[5] B. Fraass, K. Doppke, M. Hunt, G. Kutcher, G. Starkschall, R. Stern, and J. Van Dyke, "American Association of Physicists in Medicine Radiation Therapy Committee Task Group 53: quality assurance for clinical radiotherapy treatment planning.," *Med. Physics.*, vol. 25, no. 10, pp. 1773–1829, 1998.

[6] AAPM Task group 23, "Radiation treatment planning dosimetry verification: A test package prepared by task group 23 of the American Association of Physicists in Medicine," 1995.

[7] A. . Boyer and T. Schultheiss, "Effects of dosimetric and clinical uncertainty on complication-free local tumor control," *Radiother. Oncol.*, vol. 11, no. 1, pp. 65–71, 1988.

[8] K. L. Prado, S. M. Kirsner, and R. C. Erice, "Corrections to traditional methods of verifying tangential-breast 3D monitor-unit calculations: use of an equivalent triangle to estimate effective fields.," *J. Appl. Clin. Med. Phys.*, vol. 4, no. 1, pp. 51–7, Jan. 2003.

[9] I. Kay and P. Dunscombe, "Verifying monitor unit calculations for tangential breast fields," vol. 7, no. 2, pp. 50–57, 2006.

[10] I. Kay and T. Meyer, "Verifying monitor unit calculations for tangential whole breast fields in 3-dimensional planning," *J.Appl. Clin. Med. Phys.*, vol. 9, p. 2713 , 2008.

[11] G. J. Kutcher, L. Coia, M. Gillin, W. F. Hanson, S. Leibel, R. J. Morton, J. R. Palta, J. A. Purdy, L. E. Reinstein, G. K. Svensson, M. Weller, and L. Wingfield, "Comprhensive QA for radiation oncology," *Med. Phys.*, vol. 21, no. 582–618, 1994.

[12] L. Duggan, T. Kron, S. Howlett, A. Skov, and P. O'Brien, "An independent check of treatment plan, prescription and dose calculation as a QA procedure," *Radiother. Oncol.*, vol. 42, pp. 297–301.

[13] American college of Radiology, "Practice guideline for 3D external beam radiation planning and conformal therapy," *Radiat. Ther.*, 2006.

[14] K. a Gifford, D. S. Followill, H. H. Liu, and G. Starkschall, "Verification of the accuracy of a photon dose-calculation algorithm.," *J. Appl. Clin. Med. Phys.*, vol. 3, no. 1, pp. 26–45, Jan. 2002.

[15] P. M. R. Calandrino, G. M. Cattaneo, C. Fiorino, B. Longobardi and and P. Signorotto, "Detection of systematic errors in external radiotherapy before treatment delivery," 1997.

[16] G. Leunens, J. Verstraete, W. Van den Bogaert, J. Van Dam, A. Dutreix, and van der Schueren.E, "Human errors in data transfer during the preparation and delivery of radiation treatment affecting the final result: 'garbage in, garbage out'. Radiother Oncol. 1992; 23: 217-222."

[17] P. Ortiz, J. M. Cosset, O. Holmberg, J. C. Rosenwald, and P. Dunscombe, "Preventing Accidental Exposures from New External Beam Radiation Therapy Technologies," *Int. Comm. Radiol. Prot. Publ.*, vol. ICRP 39, p. 112, 2009.

[18] A. Dutreix, B. . Bjärngard, A. Bridier, B. Mijnheer, J. Shaw, and H. Svensson, "Physics for clinical radiotherapy - Monitor unit calculation for high energy photon beams," *ESTRO*, vol. Booklet No, 1997.

[19] B. Mijnheer, A. Bridier, K. Garibaldi, K. Torzsok, and J. Venselaar, "Physics for clinical radiotherapy - Monitor unit calculation for high energy photon beams - Practical examples 2001.," *ESTRO*, vol. Booklet No, 2001.

[20] R. L. Stern, R. Heaton, M. W. Fraser, T. H. Kirby, A. Molineu, and T. C. Zhu, "Verification of monitor unit calculations for non-IMRT clinical radiotherapy : Report of AAPM Task Group 114," pp. 504–530, 2011.

[21] ICRU, "Fundamental quantities and units for ionizing radiation," *ICRU Publ.*, vol. 60, 1998.

[22] A. Ahnesjö and M. M. Aspradakis, "Dose calculations for external photon beams in radiotherapy.," *Phys. Med. Biol.*, vol. 44, pp. R99–R155, 1999.

[23] Watger, "The ideal dosimeter for intensity modulated radiation therapy (IMRT)," *J. Phys.*, pp. 4–8, 2004.

[24] P. Mayles, A. Nahum, and J. . Rosenwald, *HANDBOOK OF RADIOTHERAPY PHYSICS, Theory and Practice*, 1st ed. CRC press Taylor & Francis group, 2007.

[25] E. B. Podgorsak, *Radiation Oncology Physics : A Handbook for Teachers and Students*, 1st ed. International Atomic Energy Agency, 2005.

[26] W. Bragg, "Studies in radioactivity," 1912.

[27] L. . Gray, "An ionization method for the absolute measurement of gamma-ray energy," *Proc. R. Soc. A Math. Phys. Eng. Sci.*, vol. 156, no. 889, pp. 578–596, 1936.

[28] L. V. Spencer and F. H. Attix, "A theory of cavity ionisation," *Radiat. Res.*, vol. 3, no. 3, pp. 239–254, 1955.

[29] T. Burlin, "Further examination of theories relating the absorption of gamma-ray energy in a medium to the ionization produced in a cavity," *Phys. Med. Biol.*, vol. 11, no. 2, pp. 255–266, 1966.

[30] G. Riknerf and E. Grusellt, "General specifications for semiconductors for use in radiation dosimetry," *Phys. Med. Biol.*, vol. 32, no. 9, 1986.

[31] H. E. Johns and J. R. Cunningham, *The physics of radiology*, 4th ed. Charles C Thomas publisher, 1983.

[32] F. M. Khan, *The Physics of Radiation Therapy*, 1st ed. Lippincott Williams&Wilkins, 2010.

[33] H. William R., *Radiologic Physics, Equipment and Quality Control*, 1st ed. year book medical publishers,inc., 1977.

[34] A. Niroomand-Rad, C. R. Blackwell, B. M. Coursey, K. P. Gall, J. M. Galvin, W. L. McLaughlin, a S. Meigooni, R. Nath, J. E. Rodgers, and C. G. Soares, "Radiochromic film dosimetry: recommendations of AAPM Radiation Therapy Committee Task Group 55. American Association of Physicists in Medicine.," *Med. Phys.*, vol. 25, no. 11, pp. 2093–2115, 1998.

[35] W. Sewchand, F. . Khan, and J. Williamson, "Variation in depth dose data between open and wedge fields for 4 MV X-rays.," *Radiology*, pp. 1127–789.

[36] P. Metcalfe, T. Kron, and P. Hoban, *The physics of radiotherapy X-rays and electrons*. Medical Physics publishing, 2007.

[37] I. speciality Products, "Gafchromic ®: self developing film for radiotherapy dosimetry," 2010.

[38] AGENCY INTERNATIONAL ATOMIC ENERGY, "Absorbed Dose Determination in External Beam Radiotherapy An International Code of Practice for Dosimetry Based on Standards of Absorbed Dose to Water," 2000.

[39] R. A. Peter, J. B. Peter, B. . Coursey, W. . Hanson, M. S. Huq, N. Ravinder, and D. W. . Rogers, "AAPM ' s TG-51 protocol for clinical reference dosimetry of high-energy photon and electron beams," *Med. Phys.*, vol. 26, no. 9, pp. 1847–1870, 1999.

[40] J. Van Dyk, R. B. Barnett, and J. J. Battista, "Computerized Planning Systems," pp. 231–286.

[41] F. Khan and B. Gerbi, *Treatment Planning in Radiation Oncology*, 3rd ed. Lippincott Williams&Wilkins, 2012.

[42] International Commission on Radiation units, "Determination of absorbed dose in a patient irradiated by beams of x or gamma rays in radiotherapy procedures, ICRU Report No. 24," 1976.

[43] Dutriex, Bjarngard, Bridier, Mijnheer, Shaw, and Svenson, "Monitor Unit Calculation For High Energy Photon Beams," 1997.

[44] L. Weber, "Photon Dose Calculations in a Fluence- Based Treatment Planning System Data Processing, Implementation and Validation," Lund University, 2003.

[45] L. Liang, "Development and Application of a Random Lung Model for Dose Calculations in Radiotherapy," University of Michigan, 2007.

[46] T. D. Sterling, H. Perry, and L. Katz, "Derivation of a mathematical expression for the percent depth dose surface of cobalt-60 beams and visualization of multiple field dose distributions," *Br. J. Radiol.*, vol. 37, pp. 544–550, 1964.

[47] J. Chan, D. Russell, V. G. Peters, and T. J. Farrell, "Comparison of monitor unit calculations performed with a 3D computerized planning system and independent 'hand' calculations: results of three years clinical experience.," *J. Appl. Clin. Med. Phys.*, vol. 3, no. 4, pp. 293–301, Jan. 2002.

[48] T. Knoos and L. Wittgren, "Which depth dose data should be used for dose planning when wedge filters are used to modify the photon beam?," *Phys. Med. Biol.*, vol. 36, pp. 255–267, 1991.

[49] S. Heukelom, J. H. Lanson, and B. J. Mijnheer, "Wedge factor constituents of high energy photon beams: Field size and depth dependence," *Radiother. Oncol*, vol. 30, pp. 66–73.

[50] J. P. Gibbons, J. a Antolak, D. S. Followill, M. S. Huq, E. E. Klein, K. L. Lam, J. R. Palta, D. M. Roback, M. Reid, and F. M. Khan, "Monitor unit calculations for external photon and electron beams: Report of the AAPM Therapy Physics Committee Task Group No. 71.," *Med. Phys.*, vol. 41, no. 3, pp. 031501–33, Mar. 2014.

[51] K. Gupta, S and R. Cunningham, J, "Measurement of tissue-air ratios and scatter functions for large field sizes, for cobalt 60 gamma radiation," *Br. J. Radiol.*, vol. 39, no. 457, pp. 7–11, 1966.

[52] J. . Cunningham, "Scatter-Air Ratios," *Phys. Med. Biol.*, vol. 17, no. 1, pp. 42–51, 1972.

[53] J. R. Clarkson, "A note on depth doses in fields of irregular shapes," *Br. J. Radiol.*, vol. 14, p. 255, 1941.

[54] H. Withers, "Biological aspects of conformal therapy," *Acta Oncol.*, vol. 39, no. 5, pp. 567–577, 2000.

[55] T. Schultheiss, C. Orton, and R. Peck, "Models in radiotherapy: volume effects," *Med. Phys.*, vol. 10, no. 4, pp. 410–415, 1983.

[56] J. . Lyman, "Complication probability as assessed from dose-volume histograms," *Radiat. Res. Suppl.*, vol. 8, pp. S13–S19, 1985.

[57] G. Kutcher, C. Burman, M. Brewster, and E. Al.., "Histogram reduction method for calculating complication probabilities for three-dimensional treatment planning evaluations," *Int. J. Radiat. Oncol.*, vol. 21, no. 1, pp. 137–146, 1991.

[58] P. Källman, A. Ågren, and A. Brahme, "Tumour and normal tissue responses to fractionated nonuniform dose delivery," *Int. J. Radiat. Biol.*, vol. 62, no. 2, pp. 249–262, 1992.

[59] A. Niemierko, "Reporting and analyzing dose distributions: a concept of equivalent uniform dose," *Med. Phys.*, vol. 24, no. 1, pp. 103–110, 1997.

[60] A. Niemierko, "A generalised concept of equivalent uniform dose (EUD)," *Med Phys*, vol. 26, p. 1100, 1999.

[61] A. Brahme, "Dosimetric precision requirements in radiation therapy," *Acta radiolologica.Oncology*, vol. 23, no. 5, pp. 379–391, 1984.

[62] B. J. Mijnheer, J. . Battermann, and A. Wambersie, "What degree of accuracy is required and can be achieved in photon and neutron therapy?," *Radiother. Oncol.*, vol. 8, pp. 237–52, 1987.

[63] A. Brahme, J. Chavaudra, T. Landberg, E. C. McCullough, F. Nusslin, J. A. Rawlinson, G. Svensson, and H. Svensson, *Accuracy requirements and quality assurance of external beam therapy with photons and electrons*, vol. 15(Suppl. 1988.

[64] A. Dutriex, "When and how can we improve precision in radiotherapy?," *Radiother. Oncol*, vol. 2, pp. 275–292, 1984.

[65] R. Calandrino, G. . G. M. Cattaneo, C. Fiorino, B. Longobardi, P. Mangili, and P. Signorotto, "Detection of systematic errors in external radiotherapy before treatment delivery," *Radiother. Oncol*, vol. 45, pp. 271–274, 1997.

[66] P. Andreo, "Uncertainties in dosimetric data and beam calibration," *Int. J. Radiat. Oncol. Biol. Phys.*, vol. 19, no. 1233–47, 1990.

[67] S. Johnsson, *Development and Evaluation of an Independent System for Absorbed Dose Calculations in Radiotherapy*. 2003.

[68] C. T. Baird, G. Starkschall, H. H. Liu, T. A. Buchholz, and K. R. Hogstrom, "Verification of tangential breast treatment dose calculations in a commercial 3D treatment planning system," vol. 2, no. 2, pp. 73–84, 2001.

[69] S. J. Howlett and T. Kron, "Monitor unit calculation for tangential breast treatments: verification in an anthropomorphic phantom.," *J. Appl. Clin. Med. Phys.*, vol. 3, no. 3, pp. 235–40, Jan. 2002.

[70] M. M. Ellen, K. R. Hogstrom, L. A. Miller, R. C. Erice, and T. A. Buchholz, "A comparison of 18-MV and 6-MV treatment plans using 3D dose calculation with and without heterogeneity correction," *Med. Dosim.*, vol. 24, pp. 287–294, 1999.

[71] L. J. Pierce, M. H. Stawderman, K. R. Douglas, and A. S. Lichter, "Conservative surgery and radiotherapy for early-stage breast cancer using a lung density correction," *Int. J. Radiat. Oncol., Biol.*, vol. 39, pp. 921–928, 1997.

APPENDICES

APPENDIX A

(Visual Basic for Applications (VBA) Codes developed and used in this thesis)

A.1 VBA codes to generate coordinates of contour and prescription points relative to geometry of beams in section 3.1.

The procedure reads input coordinates relative to patient geometry from the user interface and produces the coordinates relative to beam geometry through plane rotation operation.

```
'reads coordinates of points from entry cells, translates them to a coordinate system related to the geometry of beams, and displays the translated coordinates of points.
Public Function sngRotate(wrkbk As Worksheet)
Dim sngPCXs(11) As String ' an array for holding input coordinate points, 10 points on body contour and 1 prescription point
Dim sngPCYs(11) As String
Dim sngMCXs(11) As String
Dim sngLCXs(11) As String
Dim sngMCYs(11) As String
Dim sngLCYs(11) As String
Dim sngPPX As String
Dim sngPPY As String
Dim sngBPX As String
Dim sngBPY As String
Dim sngMAngle As String
Dim sngLAngle As String
Dim intXContourColumn As Integer
Dim intYcontouurcolumn As Integer
Dim inti As intger ' variable for accessing sequentially entered values in order with a loop
With wrkbk
'obtain the field angle for the medial and lateral fields from the respective entry cell on the user interface sheet
sngMAngle = .Cells(29, 4)
sngLAngle = .Cells(29, 4)
'get entered coordinates of contour points and translate them to coordinates of the tangential beam
For inti = 2 To 12
'on the user interface sheet, entry cells for X and Y coordinates of 10 measured contour points and 1 prescription points are on column 4 and column 5 respectively, from row 2 to raw 12
'the coordinates are measured relative to a coordinate system that is drawn on the paper or transverse CT slice containing the patients external contour
sngPCXs = .Cells(inti, 4)
sngPCYs = .Cells(inti, 5)
```

```
'Multiply coordinates of the entered body contour and prescription points with a rotation matrix
to express them relative to the Medial and Lateral beams coordinate system
sngMCXs = sngPCXs * Applications.cosine(sngMAngle) + sngPCYs * Applications.sine(sngMAngle)
sngMCYs = sngPCYs * Applications.cosine(sngMAngle) - sngPCXs * Applications.sine(sngMAngle)
sngLCXs = sngPCYs * Applications.cosine(sngLAngle) - sngPCXs * Applications.sine(sngLAngle)
sngLCYs = sngPCYs * Applications.cosine(sngLAngle) - sngPCXs * Applications.sine(sngLAngle)
'Display the translated coordinates on output cells on the user interface sheet
.Cells(6, inti) = sngMCXs
.Cells(7, inti) = sngMCYs
.Cells(8, inti) = sngLCXs
.Cells(9, inti) = sngLCYs
Next inti
End With
End Function
```

A.2 VBA code to compute relative scattered dose at the calculation point based on Cunningham's method of differential scatter air ratios (dSAR) in section 3.1.2.

The code takes in the translated coordinates of points on a single transverse breast contour and the dose normalization location from the code in A.1. The contour is then projected in the transverse direction to form a 3D closed breast volume with a calculation point inside of it. The total scatter maximum ratio that would be measured at the calculation point as a result of two tangential beams with given parameters irradiating the homogenous breast volume will be computed by Clarkson's sector summation of differential scatter maximum ratios.

```
Public Function sngScatterMaximumRatio(sngFieldWidth1 As Single, sngFieldWidth2 As Single,
sngSplash As Single, sngFieldLength As Single, txtEnergy As String, wrkst As Worksheet, wrkSMR
As Worksheet)

Dim wrkRange As Range
Dim intColumnOffSet As Integer 'holds the column index number where the first column of
range appears
If txtEnergy = "6MV" Then
Set wrkRange = wrkSMR.Range("six")
```

```
intColumnOffSet = 0
ElseIf txtEnergy = "15MV" Then
Set wrkRange = wrkSMR.Range("fifteen")
ElseIf txtEnergy = "Cobalt" Then
Set wrkRange = wrkSMR.Range("cobalt")
ElseIf txtEnergy = "Co15" Then
Set wrkRange = wrkSMR.Range("cobaltfif")
ElseIf txtEnergy = "Co30" Then
Set wrkRange = wrkSMR.Range("cobaltth")
ElseIf txtEnergy = "Co45" Then
Set wrkRange = wrkSMR.Range("cobaltfor")
ElseIf txtEnergy = "Co60" Then
Set wrkRange = wrkSMR.Range("cobaltsix")
intColumnOffSet = 26
End If
sngScatterMaximumRatio = sngCalculateSMR(sngFieldWidth1, sngFieldWidth2, sngSplash,
sngFieldLength, wrkRange, wrkst, intColumnOffSet)
End Function
Public Function sngCalculateSMR(sngFieldWidth1 As Single, sngFieldWidth2 As Single, sngSplash
As Single, sngFieldLength As Single, wrkRange As Range, wrkst As Worksheet, intColumnOffSet
As Integer)
Dim sngSum As Single
Dim sngAngleIndex As Single
Const sngDifferentialAngle As Single = 0.174
Dim sngRadius As Single
Dim sngBeamAngle As Single
Dim sngXCalculationPoint As Single
Dim sngYCalculationPoint As Single
Dim sngRadiusIndex As Single
Const sngDifferentialRadius As Single = 0.0625
Dim sngXRadiusIndex As Single
Dim sngYRadiusIndex As Single
Dim intColumnIndex As Integer
Const intXRowIndex As Integer = 10
Const intYRowIndex As Integer = 11
Dim sngDifferentialSAR As Single
Dim sngDepthToRadiusIndex As Single
With wrkst
sngXCalculationPoint = .Cells(22, 6)
sngYCalculationPoint = .Cells(23, 6)
sngBeamAngle = .Cells(31, 4)
End With
'initialize SMR to zero
sngSum = 0
'Divide the plane of the calculation point inside the scattering volume into sectors of width 10
degrees
For sngAngleIndex = 0.087 To 3.14 Step 0.174
```

```
'Calculate the radius from the calculation point to the edge of the scattering volume at the
indexed angle
sngRadius = sngFindRadius2(sngAngleIndex, sngFieldLength, sngFieldWidth1, sngFieldWidth2,
sngSplash, sngXCalculationPoint)
'Divide the radius in to differential elements to evaluate the depth at diffrent point on the radius
   For sngRadiusIndex = sngDifferentialRadius To sngRadius Step sngDifferentialRadius
   'Progect the the growing radial lengthes on to the x-axis of the breast contour points,
   'in order to calculate the corresponding x and y points on other planes that are-
   'parallel to the plane containing the breast contour points
   sngXRadiusIndex = SngFindXRadiusIndex2(sngXCalculationPoint, sngRadiusIndex,
sngAngleIndex)
   'Evaluate the y point corresponding to the progected x point for a given radius length
     'Check if the breast irradiated is right breast
     If sngBeamAngle > 0 And sngBeamAngle <= 90 Then
     For intColumnIndex = 2 To 11
    'Check which interval of the breast contour points is appropriate for the calculation of y
     If sngXRadiusIndex >= wrkst.Cells(intXRowIndex, intColumnIndex) Then
     sngYRadiusIndex = sngFindYRadiusIndex2(intColumnIndex, intXRowIndex, intYRowIndex,
sngXRadiusIndex, wrkst)
      Exit For
      Else
      End If
      Next intColumnIndex
      'Check if the breast is left breast
      ElseIf (sngBeamAngle >= 270 And sngBeamAngle < 360) Or sngBeamAngle = 0 Then
       'Check which interval of the breast contour points is appropriate for the calculation of y
       For intColumnIndex = 2 To 11
      If sngXRadiusIndex <= wrkst.Cells(intXRowIndex, intColumnIndex) Then
      sngYRadiusIndex = sngFindYRadiusIndex2(intColumnIndex, intXRowIndex, intYRowIndex,
sngXRadiusIndex, wrkst)
      Exit For
      Else
      End If
      Next intColumnIndex
      End If

   'Calculate the depth at the differential radius
   sngDepthToRadiusIndex = sngFindDepthToRadiusIndex2(sngYCalculationPoint,
sngYRadiusIndex)
   'Look up the SAR from the SAR table
   sngDifferentialSAR = sngFindDifferentialSAR2(sngDepthToRadiusIndex, sngRadiusIndex,
sngDifferentialRadius, wrkRange, intColumnOffSet)
   'Accumulate The SAR From the differential radius elements
   sngSum = sngSum + sngDifferentialSAR
   Debug.Print sngSum & "    " & sngRadius & "     " & sngRadiusIndex & "    " &
sngDepthToRadiusIndex
   Next sngRadiusIndex
Next sngAngleIndex
```

```
'Display the resulting total SMR on the Excel sheet Cell
sngCalculateSMR = sngSum * 2
End Function

Private Function sngFindRadius2(sngAngleIndex As Single, sngFieldLength As Single,
sngFieldWidth1 As Single, sngFieldWidth2 As Single, sngSplash As Single, sngXCalculationPoint
As Single)
   If sngAngleIndex <= Atn(0.5 * sngFieldLength / (sngFieldWidth1 - sngXCalculationPoint)) Then
   sngFindRadius2 = Abs((sngFieldWidth1 - sngXCalculationPoint) / (Cos(sngAngleIndex)))
   ElseIf sngAngleIndex <= 3.14 - Atn(0.5 * sngFieldLength / (sngXCalculationPoint +
sngFieldWidth2)) Then
   sngFindRadius2 = Abs(0.5 * sngFieldLength / Sin(sngAngleIndex))
   Else
   sngFindRadius2 = Abs((sngXCalculationPoint + sngFieldWidth2) / Cos(sngAngleIndex))
   End If
End Function



Private Function SngFindXRadiusIndex2(sngXCalculationPoint As Single, sngRadiusIndex As
Single, sngAngleIndex As Single)
Dim sngBeamAngle As Single
sngBeamAngle = Excel.Workbooks("BeamData(SGMC)").Worksheets("USER").Cells(31, 4)
If sngBeamAngle > 0 And sngBeamAngle <= 90 Then
SngFindXRadiusIndex2 = sngRadiusIndex * Cos(sngAngleIndex) + sngXCalculationPoint
ElseIf (sngBeamAngle >= 270 And sngBeamAngle < 360) Or sngBeamAngle = 0 Then
SngFindXRadiusIndex2 = sngRadiusIndex * Cos(sngAngleIndex) + sngXCalculationPoint
End If
End Function
Private Function sngFindYRadiusIndex2(intColumnIndex As Integer, intXRowIndex As Integer,
intYRowIndex As Integer, sngXRadiusIndex As Single, wrkst As Worksheet)
Dim sngSlope As Single
Dim Rate1 As Single
Dim Rate2 As Single
Dim Rate3 As Single
Dim Rate4 As Single
With wrkst
Rate1 = .Cells(intYRowIndex, intColumnIndex - 1)
Rate2 = .Cells(intYRowIndex, intColumnIndex)
Rate3 = .Cells(intXRowIndex, intColumnIndex - 1)
Rate4 = .Cells(intXRowIndex, intColumnIndex)
End With
sngSlope = (Rate2 - Rate1) / (Rate4 - Rate3)
sngFindYRadiusIndex2 = sngSlope * (sngXRadiusIndex - Rate4) + Rate2
End Function
Private Function sngFindDepthToRadiusIndex2(sngYCalculationPoint As Single, sngYRadiusIndex
As Single)
If sngYCalculationPoint <= 0 Then
```

```
sngFindDepthToRadiusIndex2 = Abs(Abs(sngYCalculationPoint) + sngYRadiusIndex)
Else
sngFindDepthToRadiusIndex2 = Abs(sngYRadiusIndex - sngYCalculationPoint)
End If
End Function
Private Function sngFindDifferentialSAR2(sngDepthToRadiusIndex As Single, sngRadiusIndex As
Single, sngDifferentialRadius As Single, wrkRange As Range, intColumnOffSet As Integer)
Dim q As Single
Dim sngLookUpSARr As Single
Dim sngLookUpSARq As Single
q = sngRadiusIndex - sngDifferentialRadius
If sngDepthToRadiusIndex > 2.5 Then
sngLookUpSARr = Application.HLookup(sngRadiusIndex, wrkRange,
(Application.Round(sngDepthToRadiusIndex, 0) + 2))
sngLookUpSARq = Application.HLookup(q, wrkRange,
Application.Round(sngDepthToRadiusIndex, 0) + 2)
ElseIf 1.5 <= sngDepthToRadiusIndex And sngDepthToRadiusIndex < 2.5 Then
sngLookUpSARr = Application.HLookup(sngRadiusIndex, wrkRange,
(Application.Round(sngDepthToRadiusIndex, 0) + 1))
sngLookUpSARq = Application.HLookup(q, wrkRange,
Application.Round(sngDepthToRadiusIndex, 0) + 1)
Else
sngLookUpSARr = Application.HLookup(sngRadiusIndex, wrkRange,
(Application.Round(sngDepthToRadiusIndex, 0) + 2))
sngLookUpSARq = Application.HLookup(q, wrkRange,
Application.Round(sngDepthToRadiusIndex, 0) + 2)
End If
sngFindDifferentialSAR2 = (sngLookUpSARr - sngLookUpSARq) * 0.028
End Function
```

A.3 VBA code developed for computing the" effective equivalent square field size (E)" in equation (3.4)

The code receives the total SMR at the calculation point as input from the code in A.2. The equivalent circle field size that has the total SMR at the input treatment depth will be looked up from SMR data tabulated for circular field sizes using linear interpolation. The effective equivalent square is then computed using equation 3.4.

```
Public Function sngFindEffectiveEqSq(sngDepth As Single, sngSMR As Single, wrkSMR As
Worksheet, txtEnergy As String)
Dim UsngEqSq As Single
Dim LsngEqSq As Single
Dim sngEffectiveEQC As Single
Dim sngEQS As Single
```

```
Dim sngSMRs(25) As String
Dim intColumn As Integer
Dim wrkRange As Range
If txtEnergy = "6MV" Then
Set wrkRange = wrkSMR.Range("six")
ElseIf txtEnergy = "15MV" Then
Set wrkRange = wrkSMR.Range("fifteen")
ElseIf txtEnergy = "Cobalt" Then
Set wrkRange = wrkSMR.Range("cobalt")
ElseIf txtEnergy = "Co15" Then
Set wrkRange = wrkSMR.Range("cobaltfif")
ElseIf txtEnergy = "Co30" Then
Set wrkRange = wrkSMR.Range("cobaltth")
ElseIf txtEnergy = "Co45" Then
Set wrkRange = wrkSMR.Range("cobaltfor")
ElseIf txtEnergy = "Co60" Then
Set wrkRange = wrkSMR.Range("cobaltsix")
Set wrkRange = wrkSMR.Range("fifteen")
End If
For intColumn = 2 To 24
sngSMRs(intColumn) = Application.VLookup(sngDepth, wrkRange, intColumn)
Next intColumn
For intColumn = 2 To 24
   If sngSMRs(intColumn) <= sngSMR And sngSMR <= sngSMRs(intColumn + 1) Then
   With wrkRange
   UsngEqSq = .Cells(1, intColumn + 1)
   LsngEqSq = .Cells(1, intColumn)
   End With
  sngEffectiveEQC = (sngSMR - sngSMRs(intColumn)) * (UsngEqSq - LsngEqSq) /
(sngSMRs(intColumn + 1) - sngSMRs(intColumn)) + LsngEqSq
   sngEQS = sngEffectiveEQC * 1.772
   Exit For
Else
End If
Next intColumn
sngFindEffectiveEqSq = sngEQS
End Function
```

A.4 VBA code to look-up dosimetric functions appropriate for calculation of MUs (or the dose at the MU calculation point) for a given tangential breast irradiation setup in section 3.1.3.

The effective equivalent square field size (passed to the code from the code in A.3 as input) and input treatment depth are used by the code to read PDD, TMR, and Sp data from Excel tables. The code reads field width, field length and treatment depth parameters entered on the user interface as input to look-up OAR and Sc data.

```
Public Function sngTissueMaximumRatio(sngEffEqSq As Single, sngDepth As Single, txtEnergy As String, wrkUser As Worksheet, wrkTMR As Worksheet)
Dim wrkRange As Range            'holds the reference to the excel TPR data range for the selected beam energy
Dim sngInterpolatedTMR As Single   ' stores the interpolated TPR from the appropriate TMR table
'For a given beam energy of read the TMR from the range containing TMR for the particular energy
If txtEnergy = "6MV" Then
Set wrkRange = wrkTMR.Range("six")
ElseIf txtEnergy = "15MV" Then
Set wrkRange = wrkTMR.Range("fifteen")
ElseIf txtEnergy = "Cobalt" Then
Set wrkRange = wrkTMR.Range("cobalt")
ElseIf txtEnergy = "Co15" Then
Set wrkRange = wrkTMR.Range("cobaltfif")
ElseIf txtEnergy = "Co30" Then
Set wrkRange = wrkTMR.Range("cobaltth")
ElseIf txtEnergy = "Co45" Then
Set wrkRange = wrkTMR.Range("cobaltfor")
ElseIf txtEnergy = "Co60" Then
Set wrkRange = wrkSMR.Range("cobaltsix")
End If
sngInterpolatedTMR = sngLookUpTMR(wrkRange, sngDepth, sngEffEqSq)
'Display the resulting TMR in the appropriate cell on the user interface
sngTissueMaximumRatio = sngInterpolatedTMR
End Function
'A function to look-up TMR from beam data tables  for a given beam energy, Depth and equivalent square field size
Public Function sngLookUpTMR(wrkRange As Range, sngDepth As Single, sngEffEqSq As Single)
If sngDepth <= 2.5 Then
sngLookUpTMR = Application.HLookup(sngEffEqSq, wrkRange, Application.Round(sngDepth, 0) + 1)
Else
sngLookUpTMR = Application.HLookup(sngEffEqSq, wrkRange, Application.Round(sngDepth, 0) + 2)
End If
End Function
```

```
Public Function sngPhantomScatterFactor(sngEffEqSq As Single, txtEnergy As String, wrkUser As Worksheet, wrkSp As Worksheet)
Dim wrkRange As Range          'holds the reference to the excel relative phantom scatter data range for the given beam energy
'For a given wedge angle of 0 degrees read the Phantom scatter factor from the spreedsheet containing Sp for open beam
If txtEnergy = "6MV" Then
Set wrkRange = wrkSp.Range("six")
ElseIf txtEnergy = "15MV" Then
Set wrkRange = wrkSp.Range("fifteen")
ElseIf txtEnergy = "Cobalt" Then
Set wrkRange = wrkSp.Range("cobalt")
ElseIf txtEnergy = "Co15" Then
Set wrkRange = wrkSp.Range("cobaltfif")
ElseIf txtEnergy = "Co30" Then
Set wrkRange = wrkSp.Range("cobaltth")
ElseIf txtEnergy = "Co45" Then
Set wrkRange = wrkSp.Range("cobaltfor")
ElseIf txtEnergy = "Co60" Then
Set wrkRange = wrkSp.Range("cobaltsix")
End If
sngPhantomScatterFactor = Application.VLookup(sngEffEqSq, wrkRange, 2)
End Function
Public Function sngCollimatorScatterFactor(sngEqSq As Single, txtEnergy As String, wrkSc As Worksheet)
Dim wrkRange As Range 'holds the reference to the excel Sc data table range for the selected beam energy
If txtEnergy = "6MV" Then
Set wrkRange = wrkSc.Range("six")
ElseIf txtEnergy = "15MV" Then
Set wrkRange = wrkSc.Range("fifteen")
ElseIf txtEnergy = "Cobalt" Then
Set wrkRange = wrkSc.Range("cobalt")
ElseIf txtEnergy = "Co15" Then
Set wrkRange = wrkSc.Range("cobaltfif")
ElseIf txtEnergy = "Co30" Then
Set wrkRange = wrkSc.Range("cobaltth")
ElseIf txtEnergy = "Co45" Then
Set wrkRange = wrkSc.Range("cobaltfor")
ElseIf txtEnergy = "Co60" Then
Set wrkRange = wrkSc.Range("cobaltsix")
End If
sngCollimatorScatterFactor = Application.VLookup(sngEqSq, wrkRange, 2)
End Function
Public Function sngOffAxisRatio(sngOCD As Single, sngDepth As Single, sngEqSq As Single, wrkOAR1 As Worksheet, wrkOAR2 As Worksheet, txtEnergy As String)
Dim wrkRange1 As Range
Dim wrkRange2 As Range
```

```
Dim sngOCR1 As Single
Dim sngOCR2 As Single
Dim sngUOCD As Single
Dim sngLOCD As Single
Dim sngUOCR1 As Single
Dim sngLOCR1 As Single
Dim sngUOCR2 As Single
Dim sngLOCR2 As Single
If txtEnergy = "6MV" Then
Set wrkRange1 = wrkOAR1.Range("six")
Set wrkRange2 = wrkOAR2.Range("six")
ElseIf txtEnergy = "15MV" Then
Set wrkRange1 = wrkOAR1.Range("fifteen")
Set wrkRange2 = wrkOAR2.Range("fifteen")
ElseIf txtEnergy = "Co" Then
Set wrkRange1 = wrkOAR1.Range("cobalt")
Set wrkRange2 = wrkOAR2.Range("cobalt")
ElseIf txtEnergy = "Co15" Then
Set wrkRange1 = wrkOAR1.Range("cobaltfif")
Set wrkRange2 = wrkOAR2.Range("cobaltfif")
ElseIf txtEnergy = "Co30" Then
Set wrkRange1 = wrkOAR1.Range("cobaltth")
Set wrkRange2 = wrkOAR2.Range("cobaltth")
ElseIf txtEnergy = "Co45" Then
Set wrkRange1 = wrkOAR1.Range("cobaltfor")
Set wrkRange2 = wrkOAR2.Range("cobaltfor")
ElseIf txtEnergy = "Co60" Then
Set wrkRange1 = wrkOAR1.Range("cobaltsix")
Set wrkRange2 = wrkOAR2.Range("cobaltsix")
End If
If sngOCD < 0 Then
   If Application.WorksheetFunction.Round(sngOCD, 0) <= sngOCD Then
   sngLOCD = Application.WorksheetFunction.Round(sngOCD, 0)
   Else
   sngLOCD = Application.WorksheetFunction.Round(sngOCD, 0) - 0.5
   End If
   sngUOCD = sngLOCD + 0.5
Else
      If Application.WorksheetFunction.Round(sngOCD, 0) >= sngOCD Then
      sngLOCD = Application.WorksheetFunction.Round(sngOCD, 0) - 0.5
      Else
      sngLOCD = Application.WorksheetFunction.Round(sngOCD, 0)
      End If
sngUOCD = sngLOCD + 0.5
End If

sngUOCR1 = Application.HLookup(sngUOCD, wrkRange1, Application.Round(sngDepth, 0) + 1)
sngLOCR1 = Application.HLookup(sngLOCD, wrkRange1, Application.Round(sngDepth, 0) + 1)
```

```
sngUOCR2 = Application.HLookup(sngUOCD, wrkRange2, Application.Round(sngDepth, 0) + 1)
sngLOCR2 = Application.HLookup(sngLOCD, wrkRange2, Application.Round(sngDepth, 0) + 1)
sngOCR1 = sngLOCR1 + (sngUOCR1 - sngLOCR1) / (sngUOCD - sngLOCD) * (sngOCD - sngLOCD)
sngOCR2 = sngLOCR2 + (sngUOCR2 - sngLOCR2) / (sngUOCD - sngLOCD) * (sngOCD - sngLOCD)
sngOffAxisRatio = (sngOCR1 + sngOCR2) / (2 * 100)
End Function
Public Function sngPercentageDepthDose(sngEffEqSq As Single, sngDepth As Single, txtEnergy
As String, wrkPDD As Worksheet)
Dim wrkRange As Range          'holds the reference to the excel PDD data range for the
selected beam energy
Dim sngInterpolatedPDD As Single   ' stores the interpolated PDD from the appropriate TMR
table
'For a given beam energy of read the PDD from the range containing TMR for the particular
energy
If txtEnergy = "6MV" Then
Set wrkRange = wrkPDD.Range("six")
ElseIf txtEnergy = "15MV" Then
Set wrkRange = wrkPDD.Range("fifteen")
ElseIf txtEnergy = "Cobalt" Then
Set wrkRange = wrkPDD.Range("cobalt")
ElseIf txtEnergy = "Co15" Then
Set wrkRange = wrkPDD.Range("cobaltfif")
ElseIf txtEnergy = "Co30" Then
Set wrkRange = wrkPDD.Range("cobaltth")
ElseIf txtEnergy = "Co45" Then
Set wrkRange = wrkPDD.Range("cobaltfor")
ElseIf txtEnergy = "Co60" Then
Set wrkRange = wrkPDD.Range("cobaltsix")
End If
sngInterpolatedPDD = sngLookUpPDD(wrkRange, sngDepth, sngEffEqSq)
'Display the resulting PDD in the appropriate cell on the user interface
sngPercentageDepthDose = sngInterpolatedPDD
End Function
```

A.5 VBA code to calculate the number of MUs required to deliver the prescribed dose to the prescription point or the dose to the MU calculation point in equations 3.6, 3.9 and 3.10.

The code receives dosimetric functions required for the calculation from the code in A.4. For calculation of MUs, prescribed dose and beam weight values are obtained from the user. For calculation of the dose at the MU calculation point, in order to validate MUs calculated with other methods, MUs calculated with the other methods are entered to the code through the user interface.

```
Public Function sngMU(sngSc As Single, sngSp As Single, sngPDD As Single, sngTMR As Single,
sngOAR As Single, wrkUser As Worksheet, txtEnergy As String)
Const dteCommissioningDate As Date = #12/12/2013#
Dim intWedgeAngle As Integer
Dim sngWedgeFactor As Single
Dim sngDecayTime As Single
Dim sngDecayFactor As Single
Const sngDr = 189.49 'Dose rate for refernce conditiong at commissioning time
Const sngISF = 1.01 'Inverse Square Factor at 100 SAD
Dim sngP As Single   'Total Prescribed dose per field per fraction
Const sngDr = 189.49 'Dose rate for refernce conditiong at commissioning time
Const sngISF = 1.01 'Inverse Square Factor at 100 SAD
Dim sngP As Single   'Total Prescribed dose per field per fraction
intWedgeAngle = wrkUser.Cells(43, 8)
If intWedgeAngle = 0 Then
sngWedgeFactor = 1
ElseIf intWedgeAngle = 15 Then
sngWedgeFactor = 0.767
ElseIf intWedgeAngle = 30 Then
sngWedgeFactor = 0.636
ElseIf intWedgeAngle = 45 Then
sngWedgeFactor = 0.487
ElseIf intWedgeAngle = 60 Then
sngWedgeFactor = 0.261
Else
MsgBox "Wrong Wedge Angle Entry"
End If
sngP = wrkUser.Cells(43, 4)
sngDecayTime = Application.WorksheetFunction.Days(Date, dteCommissioningDate)
sngDecayFactor = Exp(-1 * 0.693 * sngDecayTime / (365.25 * 5.26))
sngMU = sngP / (sngDr * sngSc * sngSp * sngTPR * sngWedgeFactor * sngOCR * sngDecayFactor)
End Function
```

Appendix B

(Computed MUs with the Excel program, and Oncentra and Prowess Panther TPSs)

Table B.1 MUs calculated with Prowess Panther TPS as part of a 3D tangential irradiation treatment plan with Co-60 beams and MUs calculated with the excel program using the TPS planned and computed treatment parameters.

Treatment Plan	MU(Excel program)	MU(with Prowess Panther)
1	1.49	1.38
2	0.96	0.93
3	1.18	1.15
4	0.74	0.71
5	1.26	1.28
6	0.99	0.97
7	1.36	1.33
8	0.76	0.75
9	1.41	1.38

Table B.2 MUs calculated with Oncentra TPS as part of a 3D tangential irradiation treatment plan with 6MV X-rays and MUs calculated with the excel program using the TPS planned and computed treatment parameters.

Treatment Plan	MU (Excel program)	MU(Oncentra)
1	0.77	0.75
2	0.22	0.22
3	1.03	1.02
4	1.31	1.36
5	0.53	0.55
6	0.97	0.95

Table B.3 MUs calculated with Oncentra TPS as part of a 3D tangential irradiation treatment plan with 15MV X-rays and MUs calculated with the excel program using the TPS planned and computed treatment parameters.

Treatment Plan	MU (Excel program)	MU (Oncentra)
1	0.84	0.87
2	1.13	1.16
3	0.82	0.83
4	1.03	1.02
5	0.50	0.49
6	0.97	0.97
7	1.52	1.49